Time-dependent mean-field theory for tunneling in electron-phonon systems

K. Yonemitsu*
International Centre for Theoretical Physics, P.O. Box 586, 34100 Trieste, Italy
(Received 20 December 1993; revised manuscript received 7 April 1994)

A semiclassical method is presented for tunneling of self-trapped states in many-body systems with electrons and phonons. An overcomplete set of Slater determinants, lattice coordinates, and lattice momenta is used to represent a functional integral. Stationary phase equations are solved numerically without any constraint on the dynamics of electrons and phonons, i.e., without the use of the adiabatic approximation. To evaluate transition amplitudes, we integrate over small fluctuations in both electronic and phonon degrees of freedom, keeping their time order correctly. This method can be applied to general electron-phonon systems and is useful when self-trapped states have complex structures in charge or spin densities and lattice displacements. The effective hopping strength is calculated for a self-trapped kink in the commensurate charge-density-wave state in one dimension. At strong coupling in the Holstein and attractive Hubbard models, where tunneling involves effectively a single tightly bound bipolaron, this method reproduces previous analytic results. New results are obtained at intermediate coupling where the kink is extended over a couple of lattice sites and for models with both electron-electron and electron-phonon interactions.

I. INTRODUCTION

Semiclassical methods are often useful to treat many-body systems. When stoichiometric broken-symmetry states of strongly correlated systems are doped with electrons or holes, they usually form polarons or bipolarons in the broad sense. They may accompany a lattice distortion, a distortion of spin order, or both of them. As far as response functions reflecting correlations of short range in length and time, a semiclassical method of inhomogeneous Hartree-Fock and random-phase approximations gives reasonably good results in a two-dimensional (2D) three-band Hubbard model,[1] a 1D two-band spinless fermion model,[2] and a two-site Peierls-Hubbard model.[3] Their limitations are discussed in Ref. 3. The above method treats only small-amplitude fluctuations around static mean-field solutions. The present work is devoted to large-amplitude deviations from them: imaginary-time-dependent solutions describing the tunneling process and small-amplitude fluctuations around them.

If the distortion and additional charge density with respect to the stoichiometry are self-trapped, their low-temperature dynamics can be described through tunneling.[4] Tunneling can be treated semiclassically once evolution is treated in imaginary time.[5] Another example of tunneling in many-body systems is self-trapping of excitons.[6] When a free-exciton state is metastable and separated from a self-trapped-exciton state by a potential barrier, a nonradiative process of trapping excitons occurs via tunneling. There is a recent semiclassical work on the possibility of small-polaron formation for an electron in a 2D lattice.[7] Low-temperature electrical conductivity of charge-density-wave (CDW) condensates is also another example because it is dominated by quantum-mechanical tunneling associated with soliton-antisoliton pair production.[8] On the other hand, the real-time dynamics of almost freely moving solitons in 1D electron and electron-phonon systems has been extensively investigated in a similar mean-field theory.[9]

Self-trapping is a consequence of many-body effects: it is determined by the balance between the itinerant nature determined by transfer integrals between neighboring atomic orbitals and the localizing nature governed by Coulomb repulsion and coupling with the lattice. Tunneling rates should be calculated with proper account of the balance and from a microscopic Hamiltonian which describes the many-body system well. In this work, the whole system is treated instead of separating it into a few degrees of freedom and a bath. In semiclassical treatments, the exponent of a tunneling rate is determined by classical paths,[10,11] so that they need to be solved with accuracy. Here, the shape of classical paths was not constrained, so that the paths really satisfy the stationary phase condition.

Time-dependent mean-field equations depend on the basis on which the functional integral is represented.[12,13] Because the functional integral is approximated by summation only over classical paths and small fluctuations around them, the appropriate basis should be used to describe classical paths. Here we use an overcomplete set of Slater determinants for electrons and lattice coordinates and momenta for phonons. Adoption of an overcomplete set with continuous variables is needed because only continuous paths contribute to the functional integral in the stationary phase approximation.[14] Then, we do not need to specify a complete and discrete set of Slater determinants consisting of plane-wave or atomic orbitals. The stationary phase condition automatically chooses a classical path close to a plane-wave Slater determinant at weak coupling, and one close to an atomic Slater determinant at strong coupling.

The reason for the use of Slater determinants is that the imaginary-time-dependent Hartree-Fock (HF) equation becomes the electronic part of the mean-

field equations.[12,13] We do not introduce Hubbard-Stratonovich auxiliary fields which lead to either Hartree, Fock, or half of the Hartree-Fock mean fields on the stationary phase.[15] We do not use Grassman variables because there is no direct way to apply the stationary phase approximation:[12] when auxiliary fields are introduced to remove the Grassman variables, it leads to the same consequence. Once Slater determinants are used, we must carefully take the continuum limit in time to maintain the correct order of fluctuation variables when integrations are performed.

The formalism based on Slater determinants is described in less detail in Refs. 12 and 13 than that based on auxiliary fields: Gaussian fluctuations which are necessary for completeness were not treated because a continuum limit in time is ill defined. We will below describe the Slater-determinant functional integral rather in detail and demonstrate how it is successfully applied to tunneling of self-trapped states. It produces accurate results, for both adiabatic and antiadiabatic cases, at strong coupling where the potential barrier is substantial. Here we consider the 1D extended Peierls-Hubbard model in the parameter space where the CDW is the ground state at half filling. We calculate the effective hopping strength of a self-trapped kink which connects the two degenerate CDW phases.

The kink is laid on a periodic potential whose period is two lattice spacings in the CDW background. We employ the dilute-instanton-gas approximation[10,11] to construct classical paths, i.e., multi-instanton solutions. This is not a unique way: a theory of spontaneous nuclear fission[16] does not rely on it, but it takes account of real-time-dependent paths in a classically allowed region and connects them to imaginary-time-dependent paths in classically forbidden regions. It is, however, tedious to extend this general treatment to a periodic-potential problem. A relation between this general treatment and the instanton technique for a double-well potential is briefly described in Ref. 13. We will derive mathematical properties of imaginary-time-dependent solutions and the relation to real-time-dependent ones more clearly than in Ref. 16.

In order to compare the present method with other theories, we calculate the prefactor through Gaussian integration over lowest-order fluctuations with respect to particle-hole excitations and phonons. In this process, particle-hole fluctuation amplitudes are regarded as independent variables, so that the orthonormality condition for single-particle wave functions is not strictly satisfied but only in the lowest order. It is equivalent to bosonization through linearization of particle-hole excitations. Indeed, if we treat *real*-time-dependent small fluctuations around the stable *static* mean-field solution in the present formalism, we obtain the same excitation modes as in the most unrestricted form of the random-phase approximation (RPA), which is called inhomogeneous HF plus RPA.[17]

The semiclassical results of the effective hopping strength for the self-trapped kink are consistent with previous analytic results. At strong coupling, bipolarons are tightly bound and interaction between them is weak. The kink is well localized and its tunneling involves essentially a single bipolaron. The effective hopping can be evaluated by the second-order perturbation theory with respect to bare electron hopping,[18,19] which shows exponential behavior with respect to coupling in the Holstein model and inversely proportional behavior in the attractive Hubbard model. These results are reproduced by the present method. Furthermore, effects of on-site and nearest-neighbor repulsions are studied. The tunneling of the kink is enhanced by on-site repulsion and suppressed by nearest-neighbor repulsion in a manner which has not been given by previous analytic treatments.

The outline of this paper is as follows. In Sec. II, a transition amplitude is represented in the functional integral. In Sec. III, the stationary phase approximation is used to derive the time-dependent mean-field equations. In Sec. IV, we describe mathematical properties and boundary conditions of the imaginary-time-dependent mean-field solutions. The reduced action is defined, whose imaginary part determines the exponent of a tunneling rate. In Sec. V, small fluctuations around the mean-field solutions are treated in the lowest order. The instanton formula for the effective hopping is briefly reviewed. In Sec. VI, we take the 1D extended Peierls-Hubbard model to present semiclassical results for the effective hopping of the self-trapped kink. Comparisons are made with the strong-coupling analysis for the Holstein and attractive Hubbard models. New results are shown for the extended Peierls-Hubbard model. In Sec. VII, we summarize the present method and discuss its validity and limitations. Appendixes include the quantization condition, the relation of the present method to the inhomogeneous HF plus RPA, and some numerical details. Part of the present work will be published elsewhere.[20]

II. FUNCTIONAL-INTEGRAL REPRESENTATION

To describe the formulation, we use a general Hamiltonian,

$$H=\sum_{i,j}T_{ij}(\{u_m\})c_i^\dagger c_j+\frac{1}{4}\sum_{i,j,l,m}\{ij|V|lm\}c_i^\dagger c_j^\dagger c_m c_l + \sum_{l,m}\tfrac{1}{2}K_{lm}u_l u_m+\sum_l\frac{1}{2M_l}p_l^2\ , \tag{2.1}$$

where $c_i^\dagger$ creates an electron, c_i annihilates it, u_i represents a lattice coordinate, and p_i stands for its conjugate momentum. The index i denotes both site and spin for electrons and both site and polarization for phonons. The parameter $T_{ij}(\{u_m\})$ is assumed to be linear in $\{u_m\}$. The electron-electron interaction parameters are antisymmetrized, $\{ij|V|lm\}=(ij|V|lm)-(ij|V|ml)$. The parameter K_{lm} denotes the spring constant between the ions at l and m, and M_l represents the mass of the ion at l.

We consider an initial state denoted by $|\phi_I\rangle|u_I\rangle$ at time t_I and a final state by $\langle u_F|\langle\phi_F|$ at time t_F. Here $|\phi_I\rangle$ and $\langle\phi_F|$ denote Slater determinants, in which a single-particle state γ has wave functions $\phi_{I\gamma}(i)$ and $\phi^*_{F\gamma}(i)$,

respectively. The symbols $|u_I\rangle$ and $\langle u_F|$ represent lattice coordinates u_{Il} and u_{Fl}, respectively. The transition amplitude

$$U_{I\to F} = \langle u_F|\langle\phi_F|e^{-\frac{i}{\hbar}H(t_F-t_I)}|\phi_I\rangle|u_I\rangle \tag{2.2}$$

is written in a functional integral form by decomposing the Hamiltonian

$$H = H_0[u] + H_M[p]\,, \tag{2.3}$$

with $H_M[p] = \sum_l p_l^2/(2M_l)$, and alternately inserting the closure relations

$$1 \propto \prod_l \prod_{i,\gamma\in\mathrm{occ}} \int du_l(t_k)d\phi_\gamma^*(i,t_k)d\phi_\gamma(i,t_k) \times e^{-\sum_{i,\gamma\in\mathrm{occ}}\phi_\gamma^*(i,t_k)\phi_\gamma(i,t_k)}|\phi_k\rangle|u_k\rangle\langle u_k|\langle\phi_k| \tag{2.4}$$

and

$$1 \propto \prod_l \prod_{i,\gamma\in\mathrm{occ}} \int dp_l(t_k)d\phi_\gamma^*(i,t_k)d\phi_\gamma(i,t_k) \times e^{-\sum_{i,\gamma\in\mathrm{occ}}\phi_\gamma^*(i,t_k)\phi_\gamma(i,t_k)}|\phi_k\rangle|p_k\rangle\langle p_k|\langle\phi_k| \tag{2.5}$$

in the Trotter formula. The symbol $|\phi_k\rangle$ denotes a Slater determinant at time t_k, in which a single-particle state γ has a wave function $\phi_\gamma(i,t_k)$ and is regarded as occupied ($\gamma \in$ occ). The symbols $|u_k\rangle$ and $|p_k\rangle$ represent lattice coordinates and momenta at time t_k, $u_l(t_k)$ and $p_l(t_k)$, respectively. Note that any state can be expanded with $|\phi_k\rangle|u_k\rangle$ or $|\phi_k\rangle|p_k\rangle$. The Slater determinant $|\phi_k\rangle$ does not depend implicitly on the lattice variables here. The relation between $|\phi_k\rangle$ and $|u_k\rangle$ in the stationary phase is later given by the time-dependent mean-field equations. If $|\phi_k\rangle$ were set to be the lowest-energy state for *each* lattice state $|u_k\rangle$ rather than expanded as above, the product $|\phi_k\rangle|u_k\rangle$ would become, in the stationary phase, a Born-Oppenheimer state where electrons are evolved adiabatically. As we will demonstrate below, $|\phi_k\rangle$ in the stationary phase is not an eigenstate of $H_0[u]$ at time t_k, but it is evolved according to the time-dependent (single-particle) Schrödinger equation. Therefore, the optimum product $|\phi_k\rangle|u_k\rangle$ is not a Born-Oppenheimer state. The difference occurs when the state is dynamic: the Slater determinant $|\phi_k\rangle$ depends not only on $|u_k\rangle$ at the equal time, but also on $|u_{k'}\rangle$ ($k' < k$). The difference between the adiabatic and present approaches has been pointed out in a different and more familiar context in Appendix H of Ref. 17.

In the Trotter formula, there appear factors

$$\langle u_{2k}|\langle\phi_{2k}|e^{-\frac{i}{\hbar}\epsilon H_M[p]}|\phi_{2k-1}\rangle|p_{2k-1}\rangle \times \langle p_{2k-1}|\langle\phi_{2k-1}|e^{-\frac{i}{\hbar}\epsilon H_0[u]}|\phi_{2k-2}\rangle|u_{2k-2}\rangle\,, \tag{2.6}$$

where $\epsilon = (t_F - t_I)/L$ with $2L$ being the number of inserted closure relations, and k runs from 1 to L. The state $|\phi_0\rangle|u_0\rangle$ is the same as $|\phi_I\rangle|u_I\rangle$ by definition, $\langle u_{2L}| = \langle u_F|$ due to the orthonormality, while $\langle\phi_{2L}|$ is not necessarily the same as $\langle\phi_F|$. Neglecting terms of order ϵ^2, the above factor (2.6) is rewritten as

$$\langle u_{2k}|p_{2k-1}\rangle\langle p_{2k-1}|u_{2k-2}\rangle\langle\phi_{2k}|\phi_{2k-1}\rangle\langle\phi_{2k-1}|\phi_{2k-2}\rangle \exp\left(-\frac{i}{\hbar}\epsilon\mathcal{H}[p_{2k-1},u_{2k-2},\phi_{2k-1}^*,\phi_{2k-2}]\right)\,, \tag{2.7}$$

where

$$\mathcal{H}[p_{2k-1},u_{2k-2},\phi_{2k-1}^*,\phi_{2k-2}] = \frac{\langle\phi_{2k-1}|H_0[u_{2k-2}]|\phi_{2k-2}\rangle}{\langle\phi_{2k-1}|\phi_{2k-2}\rangle} + H_M[p_{2k-1}]\,. \tag{2.8}$$

The single-particle wave functions $\phi_\gamma^*(i,t_k)$ and $\phi_\gamma(i,t_k)$ of the Slater determinants $\langle\phi_k|$ and $|\phi_k\rangle$ are independent variables. To make it clear, we rewrite $\phi_\gamma^*(i,t)$ and $\phi_\gamma(i,t)$ as $\phi_\gamma^{+*}(i,t)$ and $\phi_\gamma^-(i,t)$, respectively. Introducing a "normalized" bra wave function

$$\overline{\phi_\alpha^{+*}}(i,t) = \sum_{\beta\in\mathrm{occ}} [M(t)^{-1}]_{\alpha\beta}\phi_\beta^{+*}(i,t)\,, \tag{2.9}$$

where $M(t)$ is the $N_e \times N_e$ overlap matrix, $M(t)_{\alpha\beta} = \sum_i \phi_\alpha^{+*}(i,t)\phi_\beta^-(i,t)$, and N_e is the number of electrons, the electronic one-body density matrix is written in a simple form,[14]

$$\rho(t)_{ij} = \frac{\langle\phi^+(t)|c_j^\dagger c_i|\phi^-(t)\rangle}{\langle\phi^+(t)|\phi^-(t)\rangle} = \sum_{\gamma\in\mathrm{occ}} \phi_\gamma^-(i,t)\overline{\phi_\gamma^{+*}}(j,t)\,. \tag{2.10}$$

By definition, the single-particle wave functions satisfy the orthonormality condition

$$\sum_i \overline{\phi_\alpha^{+*}}(i,t)\phi_\beta^-(i,t) = \delta_{\alpha\beta}\,. \tag{2.11}$$

The products of overlaps are written, to the order of ϵ, as

$$\langle u_{2k}|p_{2k-1}\rangle\langle p_{2k-1}|u_{2k-2}\rangle \simeq \frac{1}{2\pi\hbar}\exp\left(i\epsilon/\hbar\left[\sum_l p_l(t_{2k-1})\left\{u_l(t_{2k}) - u_l(t_{2k-2})\right\}/\epsilon\right]\right)\,,$$

$$\langle\phi_{2k}^+|\phi_{2k-1}^-\rangle\langle\phi_{2k-1}^+|\phi_{2k-2}^-\rangle \simeq \langle\phi_{2k}^+|\phi_{2k}^-\rangle\langle\phi_{2k-1}^+|\phi_{2k-1}^-\rangle \exp(i\epsilon/\hbar[\langle\overline{\phi_{2k}^+}|i\hbar(|\phi_{2k}^-\rangle - |\phi_{2k-1}^-\rangle)/\epsilon + \langle\overline{\phi_{2k-1}^+}|i\hbar(|\phi_{2k-1}^-\rangle - |\phi_{2k-2}^-\rangle)/\epsilon])\,.$$

Finally, the transition amplitude is written as

$$U_{I\to F}=\int\mathcal{D}(p(t),u(t),\phi^{+*}(t),\phi^{-}(t))\exp\left(\frac{i}{\hbar}S[p(t),u(t),\phi^{+*}(t),\phi^{-}(t)]\right)\ , \tag{2.12}$$

where the measure is

$$\mathcal{D}(p(t),u(t),\phi^{+*}(t),\phi^{-}(t))=\frac{1}{\mathcal{N}}\prod_{k=1}^{L}\left[\prod_{l}dp_l(t_{2k-1})du_l(t_{2k})\right]\prod_{k=1}^{2L}\left[\prod_{i,\gamma\in\mathrm{occ}}d\phi_\gamma^{+*}(i,t_k)\right.$$
$$\left.\times d\phi_\gamma^{-}(i,t_k)e^{-\sum_{i,\gamma\in\mathrm{occ}}\phi_\gamma^{+*}(i,t_k)\phi_\gamma^{-}(i,t_k)}\langle\phi_k^{+}|\phi_k^{-}\rangle\right]\ . \tag{2.13}$$

Hereafter $\mathcal{N}$ denotes a normalization constant which generally takes different values in different equations. The action S is a functional of the paths $p(t)$, $u(t)$, $\phi^{+*}(t)$, and $\phi^{-}(t)$ defined by

$$S[p(t),u(t),\phi^{+*}(t),\phi^{-}(t)]=\int_{t_I}^{t_F}dt\left(\sum_l p_l(t)\frac{\partial}{\partial t}u_l(t)+\sum_{i,\gamma\in\mathrm{occ}}\overline{\phi_\gamma^{+*}}(i,t)i\hbar\frac{\partial}{\partial t}\phi_\gamma^{-}(i,t)\right.$$
$$\left.-\mathcal{H}[p(t),u(t),\phi^{+*}(t),\phi^{-}(t)]\right)-i\hbar\ln\left(\det\langle\phi_F|\phi^{-}(t_F)\rangle\right)\ , \tag{2.14}$$

where

$$\mathcal{H}[p(t),u(t),\phi^{+*}(t),\phi^{-}(t)]=\sum_{i,j}T_{ij}(\{u_m(t)\})\rho(t)_{ji}+\frac{1}{2}\sum_{i,j,l,m}\{il|V|jm\}\rho(t)_{ji}\rho(t)_{ml}$$
$$+\sum_{l,m}\frac{1}{2}K_{lm}u_l(t)u_m(t)+\sum_l\frac{1}{2M_l}p_l^2(t)\ . \tag{2.15}$$

The overlap $\langle\phi_F|\phi^{-}(t_F)\rangle=\langle\phi_F|\phi_{2L}^{-}\rangle$ is given by the determinant of the $N_e\times N_e$ matrix, $\sum_i\phi_{F\alpha}^{*}(i)\phi_\beta^{-}(i,t_F)$, and denoted by $\det\langle\phi_F|\phi^{-}(t_F)\rangle$. It is necessary for the gauge invariance of the action.[14]

III. STATIONARY PHASE APPROXIMATION

Time-dependent mean-field equations are derived by the stationary phase condition. By equating the variation of $S[p(t),u(t),\phi^{+*}(t),\phi^{-}(t)]$ with respect to $\phi_\gamma^{+*}(i,t)$ [not $\overline{\phi_\gamma^{+*}}(i,t)$], $\phi_\gamma^{-}(i,t)$, $p_l(t)$, and $u_l(t)$ to zero, we obtain[14]

$$i\hbar\frac{\partial}{\partial t}\phi_\gamma^{-}(i,t)=\sum_j h[\rho(t),u(t)]_{ij}\phi_\gamma^{-}(j,t)\ , \tag{3.1a}$$

$$-i\hbar\frac{\partial}{\partial t}\overline{\phi_\gamma^{+*}}(i,t)=\sum_j h[\rho(t),u(t)]_{ji}\overline{\phi_\gamma^{+*}}(j,t)\ , \tag{3.1b}$$

$$\frac{\partial}{\partial t}u_l(t)=\frac{1}{M_l}p_l(t)\ , \tag{3.1c}$$

$$\frac{\partial}{\partial t}p_l(t)=-\sum_{i,j}\bar{g}_{ij}^{l}\rho(t)_{ji}-\sum_m K_{lm}u_m(t)\ , \tag{3.1d}$$

where $\bar{g}_{ij}^{l}=\partial T_{ij}(\{u_m\})/\partial u_l$ denotes the electron-phonon coupling strength, and $h[\rho(t),u(t)]$ is the HF matrix

$$h[\rho(t),u(t)]_{ij}=T_{ij}(\{u_m(t)\})+\sum_{l,m}\{il|V|jm\}\rho(t)_{ml}\ . \tag{3.2}$$

Here we have fixed the arbitrary phases of the vectors $\langle\phi^{+}(t)|$ and $|\phi^{-}(t)\rangle$. So far, the formulation is generally applied to any Slater determinant in which single-particle states are arbitrarily occupied.

Hereafter, we consider the Slater determinant where the lowest-energy single-particle states are occupied *at the initial time*. Quantization is achieved as follows. Energy eigenvalues constitute poles and branch cuts of the trace of the resolvent operator[21]

$$G(E)\equiv\mathrm{tr}\frac{1}{E-H+i\eta}\ , \tag{3.3}$$

which can be written in the functional integral form

$$G(E)=-\frac{i}{\hbar}\int_0^\infty dTe^{iET/\hbar}\mathrm{tr}e^{-iHT/\hbar}$$
$$=-\frac{i}{\hbar}\int_0^\infty dTe^{iET/\hbar}\times\int_{\mathrm{PBC}}\mathcal{D}(p(t),u(t),\phi^{+*}(t),\phi^{-}(t))$$
$$\times\exp\left(\frac{i}{\hbar}S[p(t),u(t),\phi^{+*}(t),\phi^{-}(t)]\right)\ , \tag{3.4}$$

with periodic boundary conditions (PBC) in time direction. Mean-field solutions would dominantly contribute

to the action. Summing up contributions from a class of them yields the quantization condition. We describe the outline in Appendix A since it is a rather straightforward generalization of Refs. 12–14 for interacting electron-phonon systems. The occupied states are precisely defined in the Appendix.

We first consider small fluctuations around a stable *static* mean-field solution. Fluctuations evolve in *real* time because of the stability of the solution. The lowest-order terms of the mean-field equations constitute the RPA equation in the most unrestricted form.[17] Though the derivation of the RPA equation itself is a straightforward generalization of Ref. 22, the calculation of the RPA total energy needs attention to the continuum limit. We describe this in Appendix B so that the connection with Ref. 17 is made clear. Here, fluctuation of the single-particle wave function for an occupied state is expanded with the zeroth-order wave functions for the unoccupied and occupied states, whose components correspond to particle-hole and hole-hole fluctuations, respectively. Particle-hole fluctuations are dominant when the amplitudes are small, as easily derived from the orthonormality condition. In Gaussian integration for the total energy, the particle-hole amplitudes and their conjugate quantities are integrated over the entire complex plane, while the hole-hole amplitudes are merely suppressed. The Pauli exclusion principle is thus violated at the large-amplitude regime. However, the contribution from the large-amplitude regime is small and it does not harm the formulation whenever the average fluctuation amplitudes are small. This treatment indeed corresponds to bosonization of particle-hole excitations.

IV. BOUNCE SOLUTIONS

When discussing tunneling, we need mean-field solutions which are periodic in imaginary time $t = -i\tau$ for $-T_2/2 < \tau < T_2/2$.[16] The single-particle wave functions $\phi_\gamma^{+*}(i,t)$ and $\phi_\gamma^-(i,t)$ of the Slater determinants $\langle\phi(t)|$ and $|\phi(t)\rangle$ are independent variables so that they need *not* be complex conjugates in the stationary phase. In *real* time, they are complex conjugates on the periodic and stationary paths,[14] but it is not the case in *imaginary* time. We write the imaginary-time-dependent variables as

$$\phi_\gamma^-(i,\tau) = \phi_\gamma^-(i, t = -i\tau) , \tag{4.1a}$$

$$\overline{\phi_\gamma^{+*}}(i,\tau) = \overline{\phi_\gamma^{+*}}(i, t = -i\tau) , \tag{4.1b}$$

$$u_l(\tau) = u_l(t = -i\tau) , \tag{4.1c}$$

$$p_l(\tau) = -ip_l(t = -i\tau) . \tag{4.1d}$$

Note the factor $-i$ in Eq. (4.1d).

We consider a mean-field state self-trapped in a local minimum of the adiabatic (i.e., $p_l = 0$) HF total energy as an initial state I, and another state self-trapped in a nearest-neighbor minimum as a final state F. The imaginary-time transition amplitude is written, with single insertion of a closure relation, as

$$\langle F|\exp\left(-\frac{HT_2}{2\hbar}\right)|I\rangle = \sum_n \langle F|n\rangle\langle n|I\rangle \exp\left(-\frac{E_nT_2}{2\hbar}\right) , \tag{4.2a}$$

where n denotes energy eigenstates. It is also written in the functional-integral form as

$$\langle F|\exp\left(-\frac{HT_2}{2\hbar}\right)|I\rangle = \int_{I\to F} \mathcal{D}(p(\tau),u(\tau),\phi^{+*}(\tau),\phi^-(\tau)) \times \exp\left(-\frac{1}{\hbar}S_E[p(\tau),u(\tau),\phi^{+*}(\tau),\phi^-(\tau)]\right) , \tag{4.2b}$$

where the Euclidean action is given from Eq. (2.12) by setting $\tau = it$:

$$S_E[p(\tau),u(\tau),\phi^{+*}(\tau),\phi^-(\tau)] = \int_{-\frac{T_2}{2}}^0 d\tau \left(\sum_l p_l(\tau)\frac{\partial}{\partial\tau}u_l(\tau) + \sum_{i,\gamma\in\text{occ}} \overline{\phi_\gamma^{+*}}(i,\tau)\hbar\frac{\partial}{\partial\tau}\phi_\gamma^-(i,\tau) + \mathcal{H}[p(\tau),u(\tau),\phi^{+*}(\tau),\phi^-(\tau)] \right) - \hbar\ln\left[\det\langle\phi_F|\phi^-(0)\rangle\right] . \tag{4.3}$$

Note that the integration in Eq. (4.3) is over $-T_2/2 \le \tau \le 0$. In the expression for $\mathcal{H}[p(\tau),u(\tau),\phi^{+*}(\tau),\phi^-(\tau)]$ above, the lattice kinetic energy should be replaced by

$$\sum_l \frac{1}{2M_l}p_l^2(t = -i\tau) = -\sum_l \frac{1}{2M_l}p_l^2(\tau) .$$

The energies of the band states are obtained by comparing the two equations (4.2) in the $T_2 \to \infty$ limit.[10,11]

The time-dependent mean-field equations are

$$-\hbar\frac{\partial}{\partial\tau}\phi_\gamma^-(i,\tau) = \sum_j h[\rho(\tau),u(\tau)]_{ij}\phi_\gamma^-(j,\tau) , \tag{4.4a}$$

$$\hbar\frac{\partial}{\partial\tau}\overline{\phi_\gamma^{+*}}(i,\tau) = \sum_j h[\rho(\tau),u(\tau)]_{ji}\overline{\phi_\gamma^{+*}}(j,\tau) , \tag{4.4b}$$

$$\frac{\partial}{\partial\tau}u_l(\tau) = \frac{1}{M_l}p_l(\tau) , \tag{4.4c}$$

$$\frac{\partial}{\partial\tau}p_l(\tau)=\sum_{i,j}\bar{g}^l_{ij}\rho(\tau)_{ji}+\sum_m K_{lm}u_m(\tau)\ , \tag{4.4d}$$

with the self-consistently determined, electronic one-body density matrix

$$\rho(\tau)_{ij}=\sum_{\gamma\in\mathrm{occ}}\phi^-_\gamma(i,\tau)\overline{\phi^{+*}_\gamma}(j,\tau)\ . \tag{4.5}$$

The HF total energy is independent of imaginary time on the stationary phase with the help of the negative kinetic energy to overcome the potential barrier. Now, the lattice displacement follows the Newton equation in the inverted potential.

The single $I\to F$ tunneling process is called an instanton. The bounce solution considered here consists of an instanton for $-T_2/2\le\tau\le 0$ and an anti-instanton for $0\le\tau\le T_2/2$. For a technical reason, the bounce solution is sought instead of the instanton solution: the boundary values are determined self-consistently for a given value of T_2, but they are not known before solution. Note that, for the $I\to F$ transition, there are generally $n+1$ instantons and n anti-instantons.

The boundary conditions for the bounce solution are[23]

$$\phi^-_\gamma\left(i,\frac{T_2}{2}\right)=e^{-\lambda_\gamma}\phi^-_\gamma\left(i,-\frac{T_2}{2}\right)\ , \tag{4.6}$$

because we have fixed the phase in Eq. (4.4a), and

$$u_l\left(\frac{T_2}{2}\right)=u_l\left(-\frac{T_2}{2}\right)\ . \tag{4.7}$$

It is shown in Appendix C that λ_γ takes a real value. The single-particle states of the lowest λ_γ's, which correspond to the lowest α_γ's in real time, are regarded as occupied and summed over for the electronic one-body densities (4.5). It is convenient to set

$$\overline{\phi^{+*}_\gamma}\left(i,\frac{T_2}{2}\right)=\phi^{-*}_\gamma\left(i,-\frac{T_2}{2}\right)\ , \tag{4.8}$$

to fix the relative phase. The electronic current density and the lattice momenta become imaginary quantities when they evolve in imaginary time. To construct continuous paths which evolve in real and pure imaginary times in classically allowed and forbidden regions, respectively, these quantities must vanish at the boundary

$$p_l\left(\frac{T_2}{2}\right)=p_l\left(-\frac{T_2}{2}\right)=0\ . \tag{4.9}$$

Note that the self-trapped states can be regarded as on the boundary. For the same reason, $u_l(T_2/2)=u_l(-T_2/2)$ must take a real value there.

From the mean-field equations and the boundary conditions, we can take

$$\overline{\phi^{+*}_\gamma}(i,\tau)=\phi^{-*}_\gamma(i,-\tau)\ , \tag{4.10a}$$

$$\rho(\tau)_{ij}=\rho(-\tau)^*_{ji}\ , \tag{4.10b}$$

$$u_l(\tau)=u_l^*(-\tau)\ , \tag{4.10c}$$

$$p_l(\tau)=-p_l^*(-\tau)\ . \tag{4.10d}$$

Because the boundary values satisfy the above relations and the differential equations are of first order, these relations always hold. The HF matrices, $h[\rho(\tau),u(\tau)]$ and $h[\rho(-\tau),u(-\tau)]$, are therefore conjugate. With the variables $\{\phi^-_\gamma(i,\tau)\}$, the orthonormality condition and the electronic one-body density matrix are written as

$$\sum_i\phi^{-*}_\alpha(i,-\tau)\phi^-_\beta(i,\tau)=\delta_{\alpha\beta}\ , \tag{4.11}$$

$$\rho(\tau)_{ij}=\sum_{\gamma\in\mathrm{occ}}\phi^-_\gamma(i,\tau)\phi^{-*}_\gamma(j,-\tau)\ . \tag{4.12}$$

The quantity $W(E)=S_c[T(E)]+ET(E)$ [see Eq. (A9)] becomes purely imaginary,

$$W(E)=iW_2(E)\ , \tag{4.13}$$

where

$$\begin{aligned}W_2(E)=\int_{-\frac{T_2}{2}}^{\frac{T_2}{2}}d\tau\Bigg(&\sum_l p_l(\tau)\frac{\partial}{\partial\tau}u_l(\tau)\\&+\sum_{i,\gamma\in\mathrm{occ}}\phi^{-*}_\gamma(i,-\tau)\hbar\frac{\partial}{\partial\tau}\phi^-_\gamma(i,\tau)\Bigg)\\&+\hbar\sum_{\gamma\in\mathrm{occ}}\lambda_\gamma\ .\end{aligned} \tag{4.14}$$

Note the minus sign in $\phi^{-*}_\gamma(i,-\tau)$ above. The quantity λ_γ is defined by the boundary condition (4.6). The quantity $W_2(E)$ takes a real value, as easily derived from the relations (4.10). For different kinds of solutions, in which the path returns without retracing the instanton path, $W_2(E)$ can be complex as happens for a particle of half-integer spin.[24]

The classical contribution of *one* instanton to the Euclidean action $S_{Ec}(T_2/2)$ is given by substitution of the instanton solution into Eq. (4.3),

$$S_{Ec}\left(\frac{T_2}{2}\right)=E_{\mathrm{HF}}(T_2)\frac{T_2}{2}+\frac{1}{2}W_2[E_{\mathrm{HF}}(T_2)]\ . \tag{4.15}$$

Note that $W_2(E)$ in Eq. (4.14) is defined for the period $-T_2/2\le\tau\le T_2/2$. We will later take the $T_2\to\infty$ limit, where the HF total energy, $E_{\mathrm{HF}}(T_2)$, becomes that of the static self-trapped solution, E_{HF}.

We will mention a difference between the present paper and Ref. 16. First note that the quantity $\phi^{-*}_\gamma(i,-\tau)$ is denoted by $\phi_\gamma(i,-\tau)$ in the latter. The latter used Hubbard-Stratonovich auxiliary fields to start from the Hartree (not Hartree-Fock) equation. An adjoint operator had to be introduced to derive the equation for $\phi_\gamma(i,-\tau)$ from that for $\phi_\gamma(i,\tau)$ there. Meanwhile, we use Slater determinants for the functional integral so that we have the HF equations for both $\phi^-_\gamma(i,\tau)$ and $\phi^{-*}_\gamma(i,-\tau)$ from the beginning. In a more general situation not treated here, paths need to be connected between classically allowed and forbidden regions. This occurs when the quantization condition is imposed on tunnel-

ing paths.[12,13] It is clear in the present representation that the quantity $\overline{\phi_\gamma^{+*}}(i,t) = \phi_\gamma^{-*}(i,t)$ is connected with $\overline{\phi_\gamma^{+*}}(i,\tau) = \phi_\gamma^{-*}(i,-\tau)$ at the boundary between classically allowed and forbidden regions.

Numerical solution of the set of partial differential equations (4.4) needs some tricks. First, the boundary conditions must be satisfied. For many degrees of freedom, a classical trajectory does not generally return to the arbitrarily chosen initial point. For a given period of T_2, we must search for a self-consistent motion of electrons and phonons during $-T_2/2 \le \tau \le T_2/2$ including initial values at $\tau = -T_2/2$. For this purpose, a method introduced in Ref. 16 was used for the electronic part. For the lattice part, the initial values were determined as described in Appendix C. Second, because the bounce solution for a given value of T_2 is on a saddle point of the action functional, ordinary iteration methods fail to converge. We imposed a constraint which vanishes at the saddle point, as described in Appendix C.

V. GAUSSIAN FLUCTUATIONS

To calculate the prefactor of a tunneling rate, quantum fluctuations around the classical path must be integrated over. Hereafter $\hbar = 1$. We denote the instanton solution of Eqs. (4.4) with superscript 0 and consider

$$\phi_\gamma^-(i,\tau) = e^{-\frac{\lambda_\gamma}{T_2}\tau}[\psi_\gamma^0(i,\tau) + \eta_\gamma(i,\tau)] , \tag{5.1a}$$

$$\overline{\phi_\gamma^{+*}}(i,\tau) = e^{\frac{\lambda_\gamma}{T_2}\tau}[\overline{\psi_\gamma^{*}}^0(i,\tau) + \overline{\eta_\gamma^*}(i,\tau)] , \tag{5.1b}$$

$$u_l(\tau) = u_l^0(\tau) + v_l(\tau) , \tag{5.1c}$$

$$p_l(\tau) = p_l^0(\tau) + q_l(\tau) , \tag{5.1d}$$

for small $\eta_\gamma(i,\tau)$, $\overline{\eta_\gamma^*}(i,\tau)$, $v_l(\tau)$, and $q_l(\tau)$. Equation (4.10a) relates $\overline{\psi_\gamma^*}^0(i,\tau)$ with $\psi_\gamma^0(i,\tau)$ above. The fluctuations are expanded as in Appendix B:

$$\eta_\gamma(i,\tau) = \sum_{\alpha\in\text{unocc}} \psi_\alpha^0(i,\tau)C_{\alpha\gamma}(\tau) + \sum_{\beta\in\text{occ}} \psi_\beta^0(i,\tau)Q_{\beta\gamma}(\tau) , \tag{5.2a}$$

$$\overline{\eta_\gamma^*}(i,\tau) = \sum_{\alpha\in\text{unocc}} \overline{\psi_\alpha^*}^0(i,\tau)\overline{C_{\alpha\gamma}^*}(\tau) + \sum_{\beta\in\text{occ}} \overline{\psi_\beta^*}^0(i,\tau)\overline{Q_{\beta\gamma}^*}(\tau) , \tag{5.2b}$$

$$v_l(\tau) = \sum_\nu \frac{1}{\sqrt{2M_l\Omega_\nu}}\Gamma_\nu(l)[C_\nu(\tau) + \overline{C_\nu^*}(\tau)] , \tag{5.2c}$$

$$q_l(\tau) = \sum_\nu \sqrt{\frac{M_l\Omega_\nu}{2}}\Gamma_\nu(l)[-C_\nu(\tau) + \overline{C_\nu^*}(\tau)] , \tag{5.2d}$$

where Ω_ν and $\Gamma_\nu(l)$ are the eigenfrequency and eigenfunction of the bare phonon, determined by Eq. (B3) below. The quantities $\eta_\gamma(i,\tau)$ and $\overline{\eta_\gamma^*}(i,\tau)$ are expanded with the use of the orthonormal wave functions $\psi_\gamma^0(i,\tau)$ and $\overline{\psi_\gamma^*}^0(i,\tau)$, respectively, which are classified into the unoccupied ($\alpha \in$ unocc) and occupied ($\beta \in$ occ) ones according to the λ_γ values, $\lambda_\alpha > \lambda_\beta$. Because the "hole-hole amplitudes," $Q_{\beta\gamma}(\tau)$ and $\overline{Q_{\beta\gamma}^*}(\tau)$, are second order with respect to the "particle-hole amplitudes," $C_{\alpha\gamma}(\tau)$ and $\overline{C_{\alpha\gamma}^*}(\tau)$, due to the orthonormality condition (4.11), we neglect them as we did in Appendix B for real time. The quadratic term $S_{Eq}(T_2/2)$ is obtained straightforwardly:

$$S_{Eq}\left(\frac{T_2}{2}\right) = \frac{1}{2}\int_{-\frac{T_2}{2}}^{0} d\tau d\tau' \left[\ \overline{C^\dagger}(\tau)\tilde{C}(\tau)\ \right] \times \left\{[\Pi_E(\tau)]^{-1}\delta\right\}\begin{pmatrix} C(\tau') \\ \overline{C^*}(\tau')\end{pmatrix} \tag{5.3}$$

with $\delta = \delta(\tau - \tau')$ and

$$[\Pi_E(\tau)]^{-1} = \begin{pmatrix} \frac{\partial}{\partial\tau} + \bar{\Omega} + K_A(\tau) & K_B(\tau) \\ K_B^*(-\tau) & -\frac{\partial}{\partial\tau} + \bar{\Omega} + K_A^*(-\tau)\end{pmatrix}. \tag{5.4}$$

Here the vector $C(\tau)$ denotes

$$C(\tau) = \begin{pmatrix} C_{\alpha\beta}(\tau) \\ C_\gamma(\tau)\end{pmatrix} , \tag{5.5}$$

and satisfies the boundary condition

$$C_{\alpha\beta}\left(-\frac{T_2}{2}\right) = \overline{C_{\alpha\beta}^*}(0) = 0 , \tag{5.6a}$$

$$C_\gamma\left(-\frac{T_2}{2}\right) + \overline{C_\gamma^*}\left(-\frac{T_2}{2}\right) = C_\gamma(0) + \overline{C_\gamma^*}(0) = 0 . \tag{5.6b}$$

The vector $\tilde{C}(\tau)$ is the transpose of $C(\tau)$. The matrices $\bar{\Omega}$, $K_A(\tau)$, and $K_B(\tau)$ are defined by

$$\bar{\Omega} = \begin{pmatrix} \bar{\Omega}_{\lambda\mu;\alpha\beta} & \bar{\Omega}_{\lambda\mu;\gamma} \\ \bar{\Omega}_{\nu;\alpha\beta} & \bar{\Omega}_{\nu;\gamma}\end{pmatrix} = \begin{pmatrix} \delta_{\lambda\alpha}\delta_{\mu\beta}\frac{\lambda_\alpha - \lambda_\beta}{T_2} & 0 \\ 0 & \delta_{\nu\gamma}\Omega_\gamma\end{pmatrix} , \tag{5.7}$$

with λ_γ defined by the boundary condition (4.6),

$$K_A(\tau) = \begin{pmatrix} K_{\lambda\mu;\alpha\beta}^{A(\tau)} & K_{\lambda\mu;\gamma}^{A(\tau)} \\ K_{\nu;\alpha\beta}^{A(\tau)} & K_{\nu;\gamma}^{A(\tau)}\end{pmatrix} = \begin{pmatrix} v_{\lambda\mu\alpha\beta}^*(\tau) & g_{\lambda\mu}^\gamma(\tau) \\ g_{\alpha\beta}^{\nu*}(-\tau) & 0\end{pmatrix} , \tag{5.8a}$$

$$K_B(\tau) = \begin{pmatrix} K_{\lambda\mu;\alpha\beta}^{B(\tau)} & K_{\lambda\mu;\gamma}^{B(\tau)} \\ K_{\nu;\alpha\beta}^{B(\tau)} & K_{\nu;\gamma}^{B(\tau)}\end{pmatrix} = \begin{pmatrix} u_{\lambda\mu\alpha\beta}^*(\tau) & g_{\lambda\mu}^\gamma(\tau) \\ g_{\alpha\beta}^\nu(\tau) & 0\end{pmatrix} , \tag{5.8b}$$

where

$$v^*_{\lambda\mu\alpha\beta}(\tau) = \{\lambda\beta|V|\mu\alpha\}(\tau) , \quad (5.9a)$$

$$u^*_{\lambda\mu\alpha\beta}(\tau) = \{\lambda\alpha|V|\mu\beta\}(\tau) , \quad (5.9b)$$

$$\{\lambda\alpha|V|\mu\beta\}(\tau) = \sum_{l,a,m,b} \{la|V|mb\} \times \overline{\psi^*_\lambda}^0(l,\tau)\overline{\psi^*_\alpha}^0(a,\tau)\psi^0_\mu(m,\tau)\psi^0_\beta(b,\tau) , \quad (5.10)$$

and

$$g^\nu_{\lambda\mu}(\tau) = \sum_{i,j,l} \bar{g}^l_{ij}\overline{\psi^*_\lambda}^0(i,\tau)\psi^0_\mu(j,\tau)\frac{1}{\sqrt{2M_l\Omega_\nu}}\Gamma_\nu(l) . \quad (5.11)$$

The above matrices satisfy

$$K_A(\tau) = K^\dagger_A(-\tau) , \quad K_B(\tau) = \tilde{K}_B(\tau) ,$$

because of

$$\{\lambda\alpha|V|\mu\beta\}(\tau) = \{\mu\beta|V|\lambda\alpha\}^*(-\tau) ,$$

$$g^\nu_{\lambda\mu}(\tau) = g^{\nu*}_{\mu\lambda}(-\tau) .$$

Due to Eq. (4.10a), the Jacobian for changing the variables from those in Eq. (B12) below to the present ones is unity. The contribution of one instanton to the right hand side of Eq. (4.2b) is then formally given, through Gaussian integration, by

$$\exp\left(-E_{\rm HF}(T_2)\frac{T_2}{2} - \frac{1}{2}W_2[E_{\rm HF}(T_2)]\right) \times |\det\{\Pi_{E0}(\tau)[\Pi_E(\tau)]^{-1}\delta\}|^{-1/2} , \quad (5.12)$$

where $\Pi_{E0}(\tau)$ is for fluctuations around the stable static solution. This formula is formal because a continuum limit is ill defined.[13] Proper ordering of fluctuation variables in time must be maintained. The correct ordering is recovered once the discrete-time representation is used. Details are described in Appendix D.

It can be shown that, in the $T_2 \to \infty$ limit, there is a zero mode corresponding to translation of the instanton solution along the imaginary time. We need to treat the zero mode differently from the other modes. By transformation of a variable from the zero-mode coordinate to a collective coordinate, the factor appearing in Eq. (5.12) can be formally written as

$$|\det\{\Pi_{E0}(\tau)[\Pi_E(\tau)]^{-1}\delta\}|^{-1/2} = JK\frac{T_2}{2} , \quad (5.13)$$

where J denotes the Jacobian and K represents the $-\frac{1}{2}$th power of the determinant with the zero mode excluded divided by the determinant for the static solution. Numerically, it is easy to get the quantity JK (Appendix D).

The well-known dilute-instanton-gas approximation[10,11] leads to, in the $T_2 \to \infty$ limit,

$$\langle F|\exp\left(-\frac{HT_2}{2\hbar}\right)|I\rangle \simeq \sum_{m,n}\delta_{m-n,1}\frac{1}{m!n!}\exp\left(-\frac{E_{\rm HF}T_2}{2\hbar} - (m+n)\frac{W_2(E_{\rm HF})}{2\hbar}\right)\left(JK\frac{T_2}{2}\right)^{m+n} = \int_0^{2\pi}\frac{d\theta}{2\pi}e^{i\theta}\exp\left(-\frac{T_2}{2\hbar}(E_{\rm HF} - 2\hbar JKe^{-\frac{W_2(E_{\rm HF})}{2\hbar}}\cos\theta)\right) , \quad (5.14)$$

where $\hbar$ is retained for clarity and m and n are numbers of instantons and anti-instantons. Thus, the energies of the band states are given, through comparison with Eq. (4.2a), by

$$E_\theta = E_{\rm HF} - 2\hbar JKe^{-\frac{W_2(E_{\rm HF})}{2\hbar}}\cos\theta . \quad (5.15)$$

The HF total energy of the static self-trapped solution determines the midpoint. Since θ is regarded as a momentum,[11] the above is the same as in the 1D tight-binding model with the nearest-neighbor hopping,

$$t_{\rm eff} = \hbar JKe^{-\frac{W_2(E_{\rm HF})}{2\hbar}} . \quad (5.16)$$

The assumption here is diluteness of the instanton gas. Because the instanton density per unit imaginary time is given by $JKe^{-\frac{W_2(E_{\rm HF})}{2\hbar}}$,[10] this formula for $t_{\rm eff}$ is good as long as it is small.

VI. ONE-DIMENSIONAL EXTENDED PEIERLS-HUBBARD MODEL

In this section, we apply the semiclassical method to the 1D extended Peierls-Hubbard model:

$$H = -t\sum_{i,\sigma}(c^\dagger_{i+1\sigma}c_{i\sigma} + c^\dagger_{i\sigma}c_{i+1\sigma}) - \beta\sum_i\left(u_i - \frac{\beta}{K}\right)n_i + U\sum_i(n_{i\uparrow}-\tfrac{1}{2})(n_{i\downarrow}-\tfrac{1}{2}) + V\sum_i(n_i-1)(n_{i+1}-1) + \frac{K}{2}\sum_i u_i^2 + \frac{1}{2M}\sum_i p_i^2 , \quad (6.1)$$

where $c^\dagger_{i\sigma}$ ($c_{i\sigma}$) creates (annihilates) an electron with spin σ at site i, $n_{i\sigma} = c^\dagger_{i\sigma}c_{i\sigma}$, $n_i = \sum_\sigma n_{i\sigma}$, and u_i and p_i represent the lattice coordinate and its conjugate momentum at site i, respectively. Hereafter the spin index σ is retained for electrons. The parameter t denotes the transfer integral, β the on-site electron-phonon coupling, K the spring constant between ions, M the ionic mass, U the on-site repulsion, and V the nearest-neighbor repulsion. We call the above the Holstein model for $U = V = 0$, and the Hubbard model for $\lambda = V = 0$.

There are three important parameters concerning the dynamics of phonons relative to electrons. Nonadiabaticity is determined by the ratio of the bare phonon frequency

$$\omega = \sqrt{\frac{K}{M}} \tag{6.2a}$$

to the bare electron hopping t. The dimensionless electron-phonon coupling strength is defined by

$$\lambda = \frac{\beta^2}{Kt} . \tag{6.2b}$$

It is proportional to the usual definition appearing in the conventional theory of superconductivity since $1/t$ is proportional to the density of states at weak coupling. Another dimensionless parameter can be defined by

$$g^2 = \frac{\beta^2}{2K\omega} . \tag{6.2c}$$

The parameter g measures the multiphonon nature.[25]

Here we take such parameters that the ground state is a CDW state at half filling [i.e., $\beta^2/K - U + 2V \gtrsim 0$ (Ref. 26)]. We remove one electron from a half-filled periodic system with an odd number of sites. The system is taken long enough so that the finite-size effect does not affect the effective hopping: we found, for all ω values taken below, the size of the lattice $N = 13$ is enough for $\lambda = 2$, $N = 9$ for $\lambda = 5$, and $N = 5$ for $\lambda = 10$. For the width of an imaginary time slice $\Delta\tau$, we took up to $\omega\Delta\tau \simeq 0.2$ at the mean-field level, and further to $\omega\Delta\tau \simeq 0.1$ at the Gaussian level. For the period of the bounce solution T_2, larger values are used for the lower potential barrier, as shown below. In numerical calculations, we always set $t = 1$.

A. Phonon frequency dependence in the Holstein model

We first consider the strong-coupling case. For $t = U = V = 0$, the Hamiltonian becomes $H = \sum_i H_i$, where

$$H_i = \frac{1}{2M}p_i^2 + \frac{K}{2}\left(u_i - \frac{\beta}{K}n_i\right)^2 + g^2\omega[1 - (n_i - 1)^2] . \tag{6.3}$$

Small bipolarons are formed, each of which consists of a pair of electrons on a site with lattice distortion of $2\beta/K$. Degeneracy of the ground states is lifted in the second order with respect to t. This results in the commensurate CDW state at half filling, where a bipolaron is located on every second site. Upon removal of one electron from a half-filled periodic system with an odd number of sites, a place is created where two consecutive sites are empty, which is regarded as a kink or a soliton connecting the two degenerate CDW phases.

The kink tunnels into the neighboring equivalent positions, which are at two lattice spacings' distance (Fig. 1), so as to form a band of Bloch states. Here the charge density and the imaginary part of the electronic current density are defined by

$$\rho_i(\tau) = \sum_\sigma \rho(\tau)_{i\sigma,i\sigma} , \tag{6.4a}$$

$$j_{i+\frac{1}{2}}(\tau) = \tfrac{1}{2}\left[\rho(\tau)_{i\sigma,i+1\sigma} - \rho(\tau)_{i+1\sigma,i\sigma}\right] , \tag{6.4b}$$

respectively. We took T_2 large enough so that $E_{\rm HF}(T_2)$ and $W_2[E_{\rm HF}(T_2)]$ take almost the $T_2 \to \infty$ values, $E_{\rm HF}$ and $W_2(E_{\rm HF})$, respectively. At $\tau = -T_2/2$, the configuration of charge densities and lattice displacements is close to that of a stable static mean-field solution, where two bipolarons are located on the first and fourth sites. The kink is localized between the second and third sites. Around $\tau = -T_2/4$, which is in the middle of Fig. 1, the bipolaron on the fourth site is once broken. Then, the charge density and the lattice distortion flow on different time scales into the third site to form another bipolaron there. Effectively, the bipolaron is shifted from the fourth to the third site and the kink is shifted from the 2–3 to the 4–5 sites. At $\tau = 0$, the configuration is close to that of another static solution. The motion after $\tau = 0$ is related to that before $\tau = 0$ by Eqs. (4.10). The quantities $j_{i+\frac{1}{2}}(\tau)$ and $p_l(\tau)$ are finite locally in space and time, and they are odd functions with respect to τ because all the quantities in Eqs. (4.10) are real here.

When the quantities near the kink are closely looked at, the difference in the electronic and phonon time scales is evident [Fig. 2(a)]. Here are shown the quantities on the third site of Fig. 1. The charge density varies more rapidly than the lattice displacement at $\tau = -T_2/4$. Because the whole motion must be periodic in time, the lattice displacement starts moving earlier than the charge density and finishes moving later. Thus, at time distant from $\tau = \pm T_2/4$, the motion of the lattice displacement is faster than that of the charge density.

Evolution of partial energies is shown in Fig. 2(b). Here, the lattice potential energy is defined by

$$\frac{K}{2}\sum_i u_i^2(\tau) , \tag{6.5a}$$

the lattice kinetic energy by

$$-\frac{1}{2M}\sum_i p_i^2(\tau) , \tag{6.5b}$$

and the electronic part of the total energy (for $U = V = 0$) by

$$-t\sum_{i,\sigma}[\rho(\tau)_{i\sigma,i+1\sigma} + \rho(\tau)_{i+1\sigma,i\sigma}]$$

$$-\beta\sum_{i,\sigma}\left(u_i(\tau) - \frac{\beta}{K}\right)\rho(\tau)_{i\sigma,i\sigma} . \tag{6.5c}$$

During the tunneling process, the amplitude of the lattice alternation decreases locally. This lowers the lattice potential energy and raises the site potential experienced by electrons. Note that the total energy is conserved: the potential barrier is overcome with the help of the negative kinetic energy. The electronic part of the total energy also varies on the time scale of the lattice displacement in Fig. 2(a). The lattice time scale determines the width of an instanton.

Evolution of the scaled lattice displacement $Ku_i(\tau)/\beta$ on the ith site into which the bipolaron tunnels is ap-

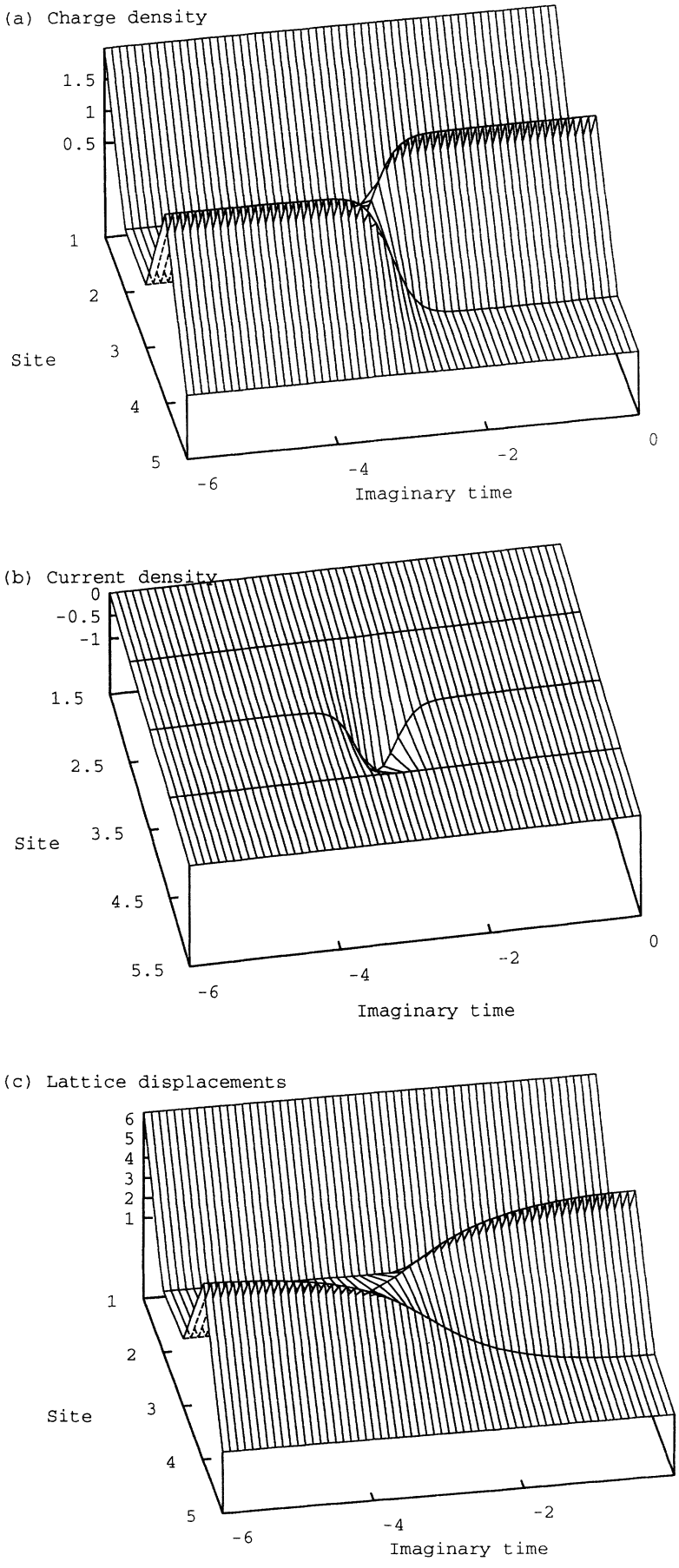

FIG. 1. Evolution in imaginary time, $-T_2/2 \leq \tau \leq 0$ ($T_2 = 12$), of (a) the charge density $\rho_i(\tau)$; (b) the imaginary part of the electronic current density $j_{i+\frac{1}{2}}(\tau)$; (c) the lattice displacements $u_i(\tau)$; and (d) the imaginary parts of the lattice momenta $p_i(\tau)$. Parameters are $\lambda = 10$, $\omega = 1$, and $U = V = 0$. Four electrons form two bipolarons on the five sites shown.

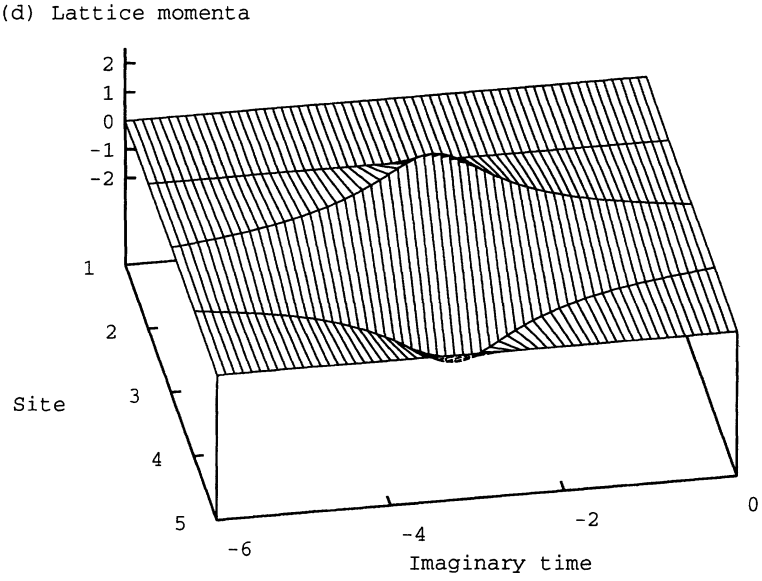

FIG. 1. (*Continued*).

proximately given by

$$\frac{K u_i(\tau)}{\beta} \simeq 1 + \tanh\left(\frac{\tau + T_2/4}{\tau_p}\right) , \tag{6.6a}$$

and that of the charge density $\rho_i(\tau)$ on the same site by

$$\rho_i(\tau) \simeq 1 + \tanh\left(\frac{\tau + T_2/4}{\tau_e}\right) . \tag{6.6b}$$

Here, τ_p and τ_e represent their respective time scales. Thus, the τ derivatives, $K\dot{u}_i(\tau)/\beta$ and $\dot{\rho}_i(\tau)$, at $\tau = -T_2/4$, which are listed in Table I, approximately give the inverse of the time scales. As ω increases, the lattice displacement moves faster, letting the motion of the charge density become still faster. The ratio of $K\dot{u}_i(\tau)/\beta$ to $\dot{\rho}_i(\tau)$ at $\tau = -T_2/4$ increases with ω and it becomes unity in the $\omega \to \infty$ limit. The instanton width becomes smaller, but it does not vanish.

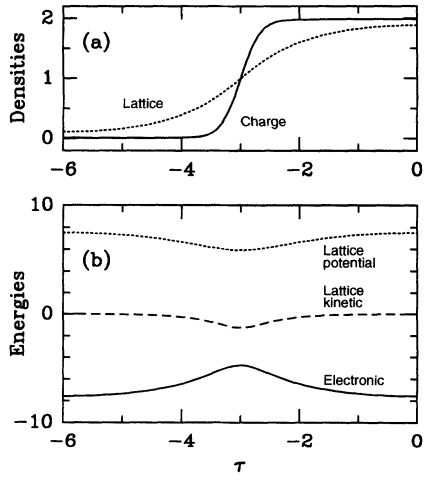

FIG. 2. Evolution in imaginary time, $-T_2/2 \leq \tau \leq 0$ ($T_2 = 12$), of (a) the charge density $\rho_i(\tau)$ and the scaled lattice displacement $K u_i(\tau)/\beta$, on the ith site into which the bipolaron tunnels; and (b) the lattice potential energy, the lattice kinetic energy, and the electronic part of the total energy. Parameters are $\lambda = 10$, $\omega = 1$, and $U = V = 0$.

We digress from the semiclassical study for a while, calculating variational wave functions and evaluating the electron-phonon correlations. We transform the 1D Holstein model by a Lang-Firsov-type transformation, $e^{S_1} H e^{-S_1}$, where

$$S_1 = -g \sum_i \left(\bar{\gamma}_i + \sum_\sigma \gamma_{i\sigma} n_{i\sigma}\right)(b_i^\dagger - b_i) , \tag{6.7a}$$

and further by a squeezing transformation,[25,27,28]

$$\tilde{H} = e^{S_2} e^{S_1} H e^{-S_1} e^{-S_2} , \tag{6.7b}$$

where

$$S_2 = -\sum_i \alpha_i (b_i^{\dagger 2} - b_i^2) , \tag{6.7c}$$

allowing variational parameters $\bar{\gamma}_i$, $\gamma_{i\sigma}$, and α_i to depend on site (and spin). The operators are transformed as

$$e^{S_1} b_i e^{-S_1} = b_i + g\left(\bar{\gamma}_i + \sum_\sigma \gamma_{i\sigma} n_{i\sigma}\right) , \tag{6.8a}$$

TABLE I. ω dependence of $K\dot{u}_i(\tau = -T_2/4)/\beta$, $\dot{\rho}_i(\tau = -T_2/4)$, their ratio, and the variational parameter $\gamma_{i\sigma}$, on the ith site where the kink is located. Parameters are $\lambda = 10$ and $U = V = 0$.

ω	$K\dot{u}_i(\tau)/\beta$	$\dot{\rho}_i(\tau)$	Ratio	$\gamma_{i\sigma}$
1	0.79	2.8	0.28	0.050
2	1.46	4.0	0.37	0.100
5	3.0	5.7	0.53	0.24
∞[a]	4.5	4.5	1.0	1.0

[a]This row is obtained from the equivalent attractive Hubbard model.

$$e^{S_1} c_{i\sigma} e^{-S_1} = c_{i\sigma} \exp[g\gamma_{i\sigma}(b_i^\dagger - b_i)] , \tag{6.8b}$$

$$e^{S_2}(b_i^\dagger \pm b_i)e^{-S_2} = (b_i^\dagger \pm b_i)e^{\pm 2\alpha_i} . \tag{6.8c}$$

Minimizing the expectation value of $\tilde{H}$ for the product of a Slater determinant and the phonon vacuum, we obtain the relations

$$\bar{\gamma}_i = \sum_\sigma (1 - \gamma_{i\sigma})\langle n_{i\sigma}\rangle , \tag{6.9a}$$

$$\gamma_{i\sigma} = \omega \left[\omega + \frac{te^{-4\alpha_i} b_{i\sigma}}{2\langle n_{i\sigma}\rangle(1 - \langle n_{i\sigma}\rangle)}\right]^{-1} , \tag{6.9b}$$

$$e^{-4\alpha_i} = \omega \left[\omega^2 + 2g^2\omega t \sum_\sigma \gamma_{i\sigma}^2 b_{i\sigma}\right]^{-\frac{1}{2}} , \tag{6.9c}$$

where

$$b_{i\sigma} = \delta_{i-1,i,\sigma}\langle c_{i\sigma}^\dagger c_{i-1\sigma} + c_{i-1\sigma}^\dagger c_{i\sigma}\rangle + \delta_{i,i+1,\sigma}\langle c_{i+1\sigma}^\dagger c_{i\sigma} + c_{i\sigma}^\dagger c_{i+1\sigma}\rangle , \tag{6.10}$$

$$\delta_{i,j,\sigma} = \exp\left[-\frac{g^2}{2}(\gamma_{i\sigma}^2 e^{-4\alpha_i} + \gamma_{j\sigma}^2 e^{-4\alpha_j})\right] , \tag{6.11}$$

and the HF equation depending on the above parameters. They are solved numerically. In the nonmagnetic case considered here, $\gamma_{i\sigma}$ is independent of spin σ. The scaled lattice distortion is given by

$$\frac{K\langle u_i\rangle}{\beta} = \bar{\gamma}_i + \sum_\sigma \gamma_{i\sigma}\langle n_{i\sigma}\rangle = \langle n_i\rangle , \tag{6.12}$$

where $\bar{\gamma}_i$ represents a component which is uncorrelated with the electronic state and $\gamma_{i\sigma}$ stands for the extent of a correlation between electrons and phonons. At half filling,[27] as the parameter changes from the adiabatic ($\omega \to 0$) to antiadiabatic ($\omega \to \infty$) limits, the nature of the lattice distortion changes from $\bar{\gamma}_i$-dominant to $\gamma_{i\sigma}$-dominant correlations. In the former, the lattice is uncorrelated with the motion of electrons. In the latter, it follows the motion completely. This holds for the doped systems considered here. The quantity $\gamma_{i\sigma}$ increases with ω as shown in the rightmost column of Table I.[29] Now, it is reasonable to regard the ratio of $K\dot{u}_i(\tau)/\beta$ to $\dot{\rho}_i(\tau)$ in the semiclassical study as a measure of the electron-phonon correlation: its behavior and that of $\gamma_{i\sigma}$ show similarity. When the ratio is far from unity, the retardation of phonons is important so that the model cannot be described by the attractive Hubbard model.

The imaginary part of the reduced action, $W_2[E_{\rm HF}(T_2)]/(2\hbar)$, and the HF total energy relative to that of the static solution, $E_{\rm HF}(T_2) - E_{\rm HF}$, vary with the period T_2 as shown in Fig. 3. Note the $T_2 \to \infty$ limit of $W_2[E_{\rm HF}(T_2)]/(2\hbar)$ determines the exponent of the effective hopping. It decreases as ω increases [Fig. 3(a)]. The quantity $W_2[E_{\rm HF}(T_2)]$ has contributions from the lattice motion [the first term in the parentheses of Eq. (4.14)] and from the electronic motion [the rest of Eq. (4.14)].

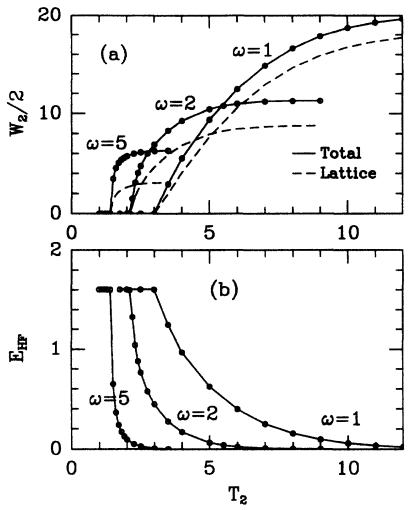

FIG. 3. (a) $W_2[E_{\rm HF}(T_2)]/(2\hbar)$ and (b) $E_{\rm HF}(T_2) - E_{\rm HF}$, for different ω values. Parameters are $\lambda = 10$ and $U = V = 0$. The lattice contribution to $W_2[E_{\rm HF}(T_2)]/(2\hbar)$ is also shown in (a).

Here shows also the lattice contribution to $W_2[E_{\rm HF}(T_2)]$. As ω increases, the electronic contribution becomes more substantial. It should be noted that the electronic contribution is not always negligible in the $\omega \to 0$ limit. It plays a decisive role in quantization of the molecular pseudorotation of Na_3,[30] through the adiabatic sign change.[31] (Recall that the quantization condition is written with the reduced action as shown in Appendix A.) The magnitude of the lattice kinetic energy at $\tau = \pm T_2/4$ is smaller than the barrier height (Table II). The discrepancy is due to contribution from electrons to the total kinetic energy, so that it increases with ω.

The HF total energy $E_{\rm HF}(T_2)$ is a decreasing function of the period T_2 [Fig. 3(b)]. In the $T_2 \to \infty$ limit, the bounce solution starts from the state identical with the stable static solution. The HF total energy $E_{\rm HF}(T_2)$ becomes that of the static solution $E_{\rm HF}$. The latter quantity is already subtracted from the former in Fig. 3(b). For finite T_2, the bounce solution starts from a higher-energy state on a small but finite slope of the potential. As T_2 approaches a critical value T_{2c} from above, $E_{\rm HF}(T_2)$ rapidly increases toward that of an *unstable* static solution on the top of the barrier. Below T_{2c}, there is no time-dependent solution so that $W_2[E_{\rm HF}(T_2)] = 0$. The flat part to the left of Fig. 3(b) thus represents the barrier height, $E_{\rm HF}(T_2 < T_{2c}) - E_{\rm HF}(T_2 = \infty)$. Infinitesimally above T_{2c}, the bounce solution corresponds to a small-amplitude harmonic oscillation around the unsta-

TABLE II. ω dependence of the absolute value of the lattice kinetic energy at $\tau = \pm T_2/4$ and the barrier height $E_{\rm HF}(T_2 < T_{2c}) - E_{\rm HF}$. Parameters are $\lambda = 10$ and $U = V = 0$.

ω	Max |lattice kinetic energy|	Barrier height
1	1.26	1.60
2	1.06	1.60
5	0.75	1.60

ble static solution, which has a characteristic period of T_{2c}. As ω increases, the instanton width becomes shorter, so that T_{2c} becomes smaller and the quantities in Fig. 3 approach faster to the values in the $T_2 \to \infty$ limit.

The absolute value of the exponent of the effective hopping, $W_2(E_{\rm HF})/(2\hbar)$, varies with ω as shown in Fig. 4. At strong coupling, bipolarons are tightly bound and the kink is well localized. Only a single bipolaron effectively participates in the tunneling as in Fig 1. In this case, the effective hopping can be evaluated by the second-order perturbation theory with respect to t.[18,19] Intermediate states have two consecutive singly occupied sites with phonons excited around the equilibrium position β/K:

$$\tilde{t} = \frac{2t^2}{\omega} \sum_{n,n'} \frac{\langle +0|n\rangle\langle n|-0\rangle\langle -0|n'\rangle\langle n'|+0\rangle}{n+n'+2g^2} , \quad (6.13)$$

where $|+0\rangle$ and $|-0\rangle$ denote the ground states of the oscillator with equilibrium positions $2\beta/K$ and 0, respectively, and $|n\rangle$ denotes the nth excited state of the oscillator centered at β/K. With the use of the well-known formula for the overlap between displaced phonon wave functions, $\tilde{t}$ is given by

$$\tilde{t} = \frac{2t^2}{\omega} e^{-2g^2} \sum_m \frac{(-2g^2)^m}{m!(m+2g^2)} . \quad (6.14)$$

For large g, it can be decomposed into an exponential and a prefactor,

$$\tilde{t} = \frac{2t^2}{\omega} F(g^2) e^{-4g^2} , \quad (6.15)$$

where $F(g^2)$ is a slowly varying function of g^2. The quantity $-\ln(\tilde{t})$ is also shown in Fig. 4 for comparison, though we need the prefactor to complete the calculation of $-\ln(t_{\rm eff})$.

The prefactor of the effective hopping, $\hbar JK$, is calculated as described in Appendix D. Compared with the calculation of $W_2(E_{\rm HF})/(2\hbar)$, smaller $\Delta\tau = T_2/L$ (as defined in Appendix C) and larger T_2 are necessary to get convergent results of $\hbar JK$. The calculation of $\hbar JK$ is less accurate than that of $W_2(E_{\rm HF})/(2\hbar)$, and the error estimation is harder. As ω decreases, the instanton density becomes exponentially small and fluctuations around the instanton solution become small as $\hbar JK$ does. Thus, the dilute-instanton-gas approximation works better. Numerically, however, the instanton width becomes longer so that necessary memory or numerical error increases. The quantity JK is roughly proportional to ω:

$$JK \simeq \omega , \quad (6.16)$$

for $\lambda = 10$ [Fig. 5(a)], though the points for $\omega = 1$ and $\omega = 2$ here are not so accurate as the size of the points indicates.

Finally, the quantity $-\ln(t_{\rm eff})$ is plotted in Fig. 5(b) and compared with the strong-coupling result $-\ln(\tilde{t})$. The semiclassical method reproduces the correct exponential behavior (6.15) at large g.

B. Coupling dependence in the Holstein model

At weak coupling, bipolarons are loosely bound and the CDW has a smaller amplitude. The kink is delocalized with a coherence length of about v_F/Δ where v_F is the Fermi velocity of the noninteracting system and Δ is a gap in the electronic spectrum at half filling. Because of the weaker binding of bipolarons, the barrier between the stable static mean-field solutions is lowered. In other words, it costs less energy to break up a bipolaron. It reduces the velocities at $\tau = \pm T_2/4$. Thus the instanton width becomes longer. The lattice displacement can follow more closely the slowed-down motion of the charge density (Table III). Note that the relation between the ratio of $K\dot{u}_i(\tau)/\beta$ to $\dot{\rho}_i(\tau)$ at $\tau = \pm T_2/4$ and the variational parameter $\gamma_{i\sigma}$ is similar to that in Table I. The ω dependence and the λ dependence are understood in a unified way when we consider them as the g dependence. Tables I and III both show the cases for $g^2 = 1$, 2.5, and 5. For the same g value, the phonon dynamics relative

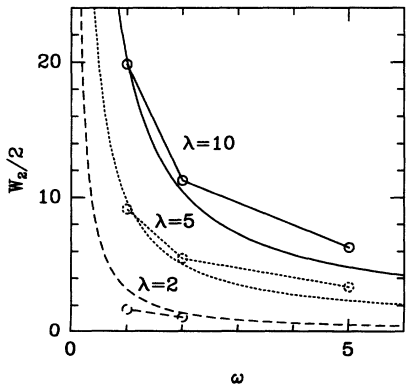

FIG. 4. $W_2(E_{\rm HF})/(2\hbar)$, as a function of ω for different λ values. Parameters are $U = V = 0$. The lines connecting the points are guides to the eye. The smooth lines show the strong-coupling results, $-\ln(\tilde{t}) \simeq 4g^2 = 2\lambda t/\omega$.

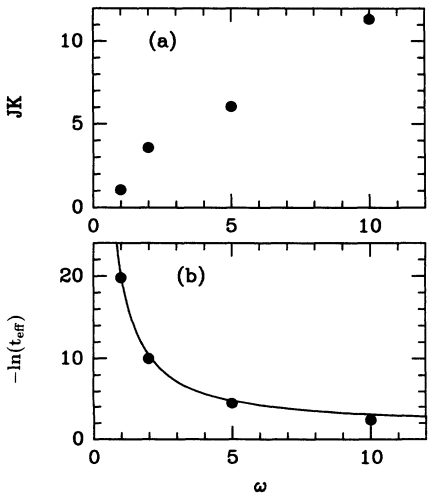

FIG. 5. (a) Prefactor $\hbar JK$ and (b) $-\ln(t_{\rm eff})$, as functions of ω. Parameters are $\lambda = 10$ and $U = V = 0$. The line in (b) shows the strong-coupling result, $-\ln(\tilde{t}) \simeq 4g^2$.

TABLE III. λ dependence of $K\dot{u}_i(\tau = -T_2/4)/\beta$, $\dot{\rho}_i(\tau = -T_2/4)$, their ratio, and the variational parameter $\gamma_{i\sigma}$, on the ith site where the kink is located. Parameters are $\omega = 1$ and $U = V = 0$.

λ	$K\dot{u}_i(\tau)/\beta$	$\dot{\rho}_i(\tau)$	Ratio	$\gamma_{i\sigma}$
2	0.35	0.52	0.67	0.26
5	0.68	1.72	0.39	0.101
10	0.79	2.8	0.28	0.050

to the electronic one [the ratio of $K\dot{u}_i(\tau)/\beta$ to $\dot{\rho}_i(\tau)$ and $\gamma_{i\sigma}$] is similar even if λ and ω values are different.

The longer instanton width results in larger T_{2c} and slower saturation of the quantities in Fig. 6 for smaller λ. Recall that the imaginary-time evolution corresponds to the real-time one in the inverted potential, and that the HF total energy $E_{\rm HF}(T_2)$ is a constant of motion. The reduced barrier height [Fig. 6(b)] means the reduced potential energy at the initial time. Therefore, it decreases the magnitude of the kinetic energy at $\tau = \pm T_2/4$ as well as the magnitude of purely imaginary velocities (i.e., the electronic current density and the lattice momenta). It results in the decrease of $W_2(E_{\rm HF})/(2\hbar)$ [Fig. 6(a)] and the increase of $t_{\rm eff}$. The electronic contributions to the reduced action and the total kinetic energy are evident in Fig. 6(a) and Table IV, respectively.

The quantities $W_2(E_{\rm HF})/(2\hbar)$ and $-\ln(\tilde{t})$ vary with λ in a similar manner, as shown in Fig. 7, though we need $\hbar JK$ to complete the calculation of $-\ln(t_{\rm eff})$. The prefactor $\hbar JK$ decreases at weak coupling [Fig. 8(a)]. It is almost inversely proportional to T_{2c}:

$$JK \simeq \frac{11}{T_{2c}}\,, \tag{6.17}$$

for $\omega = 2$ [compare Figs. 6 and 8(a)]. Finally, the quantities $-\ln(t_{\rm eff})$ and $-\ln(\tilde{t})$ are compared in Fig. 8(b).

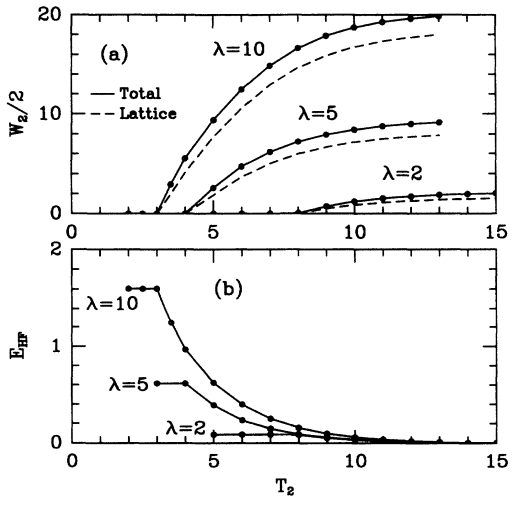

FIG. 6. (a) $W_2[E_{\rm HF}(T_2)]/(2\hbar)$ and (b) $E_{\rm HF}(T_2) - E_{\rm HF}$, for different λ values. Parameters are $\omega = 1$ and $U = V = 0$. The lattice contribution to $W_2[E_{\rm HF}(T_2)]/(2\hbar)$ is also shown in (a).

TABLE IV. λ dependence of the absolute value of the lattice kinetic energy at $\tau = \pm T_2/4$ and the barrier height $E_{\rm HF}(T_2 < T_{2c}) - E_{\rm HF}$. Parameters are $\omega = 1$ and $U = V = 0$.

λ	Max |lattice kinetic energy|	Barrier height
2	0.059	0.087
5	0.46	0.62
10	1.26	1.60

The semiclassical results would be closer to the strong-coupling results for $\omega < 2$ [see Fig. 5(b)], though the numerical calculation of $\hbar JK$ becomes more difficult.

C. Attractive Hubbard model

The Holstein model is reduced, in the $\omega \to \infty$ limit, to the attractive Hubbard model of coupling strength $U_{\rm eff} = -\beta^2/K$.[19] The imaginary-time evolution of electronic densities, $\rho_i(\tau)$, $j_{i+\frac{1}{2}}(\tau)$, etc. in the latter is therefore similar to that in the former with large ω. When the Holstein model with $\lambda = 10$ and $\omega = 5$ in Sec. VI A is compared with the attractive Hubbard model with $U = -10$ (corresponding to $\lambda = 10$ and $\omega = \infty$), the charge density of the latter changes more rapidly than the scaled lattice displacement of the former at $\tau = \pm T_2/4$. But it changes more slowly than the charge density of the former at the same time (Table I shows this result of the attractive Hubbard model in the last row).

In the antiadiabatic limit of Eqs. (4.4c) and (4.4d) for the Holstein model, $M_l \to 0$, $p_l(\tau) \to 0$, and the right hand side of Eq. (4.4d) vanishes. The lattice displacements follow the change of the charge density instantaneously and completely: their time scales are the same. For $\omega = 5$, the charge density has to move faster than the $\omega \to \infty$ limit to drag phonons, but the whole motion determined by the lattice is still slower.

The quantity $W_2(E_{\rm HF})/(2\hbar)$ increases with $|U|$ [Fig. 9(a)]. Its behavior is consistent with Figs. 4 and 7 for large ω. Because the absolute value of the exponent is small here, the behavior of the prefactor is equally impor-

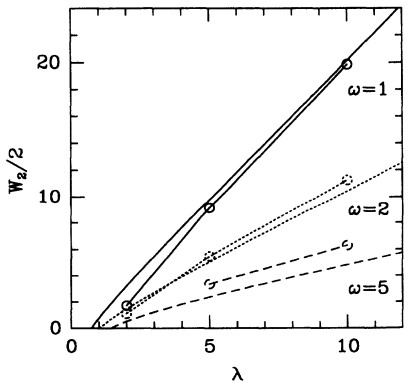

FIG. 7. $W_2(E_{\rm HF})/(2\hbar)$, as a function of λ for different ω values. Parameters are $U = V = 0$. The lines connecting the points are guides to the eye. The smooth lines show the strong-coupling results, $-\ln(\tilde{t}) \simeq 4g^2 = 2\lambda t/\omega$.

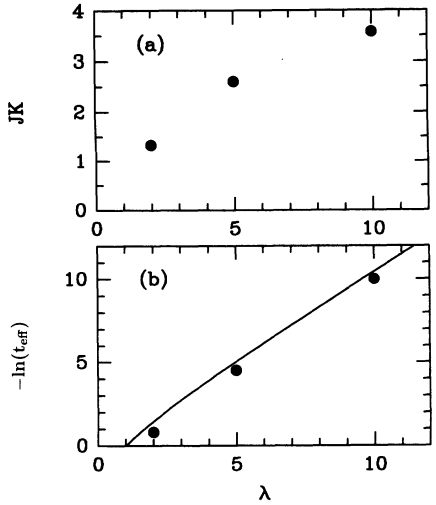

FIG. 8. (a) Prefactor $\hbar JK$ and (b) $-\ln(t_{\rm eff})$, as functions of λ. Parameters are $\omega = 2$ and $U = V = 0$. The line in (b) shows the strong-coupling result, $-\ln(\tilde{t}) \simeq 4g^2$.

tant for the effective hopping. The quantity $\hbar JK$ varies with $|U|$ as shown in Fig. 9(b). For large $|U|$, it increases with the coupling as in Fig. 8(a), partially compensating the decrease of the exponential function. At strong coupling, bipolarons are again tightly bound, the kink is well localized, and the second-order perturbation theory

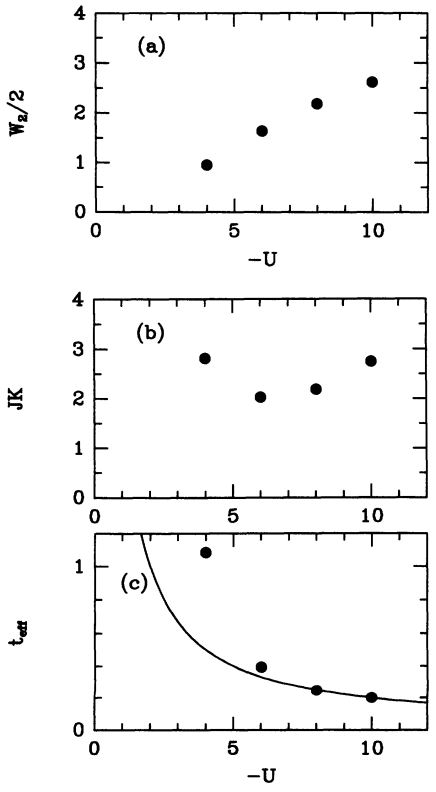

FIG. 9. (a) $W_2(E_{\rm HF})/(2\hbar)$, (b) $\hbar JK$, and (c) $t_{\rm eff}$, as functions of $|U|$. Parameters are $\lambda = V = 0$. The line in (c) shows the strong-coupling result, $\tilde{t} = 2t^2/|U|$.

with respect to t becomes relevant for the effective hopping. We define $\tilde{t}$ by the perturbational result obtained by summing the contributions from the two intermediate states,

$$\tilde{t} = \frac{2t^2}{|U|} . \tag{6.18}$$

This is obtained also by taking the $\omega \to \infty$ limit of Eq. (6.14). The quantities $t_{\rm eff}$ and $\tilde{t}$ are shown in Fig. 9(c) on a linear scale. Calculating both the exponent and the prefactor, we can reproduce the inversely proportional behavior of the effective hopping at strong coupling by the present semiclassical method.

D. Extended Peierls-Hubbard model

Here we study the effects of electron-electron interactions on the effective hopping of the kink in the Holstein model at strong coupling. In view of the fact that the effective attraction strength is given by

$$U_{\rm eff} = -\beta^2/K + U \tag{6.19}$$

in the $\omega \to \infty$ limit, and that the phase diagram in the half-filled case is divided by

$$2V = -\beta^2/K + U \tag{6.20}$$

for $t = 0$, it is conjectured for $V = 0$ that[32]

$$t_{\rm eff} \propto \exp\left[-\frac{2}{\omega}(\beta^2/K - U)\right] . \tag{6.21a}$$

On the other hand, the exponential behavior of $\tilde{t}$ for the Holstein model is determined simply by the overlaps between the displaced phonon wave functions.[33] The

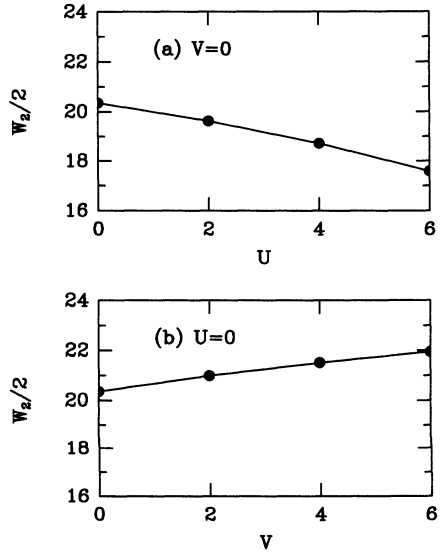

FIG. 10. $W_2(E_{\rm HF})/(2\hbar)$ (a) as a function of U for $V = 0$; and (b) as a function of V for $U = 0$. Parameters are $\lambda = 10$ and $\omega = 1$. The line is a guide to the eye.

overlaps are determined by the distance β/K between the centers of the oscillators for different occupancies. This quantity, however, does not depend on U or V for $t = 0$. Therefore, the effective hopping should not depend on U so strongly as Eq. (6.21a), but it should remain near

$$t_{\rm eff} \propto \exp\left[-\frac{2\beta^2}{\omega K}\right] , \tag{6.21b}$$

for small and finite t. For finite t, the CDW amplitude is decreased by U and increased by V. Consequently, the effective hopping is enhanced by U and suppressed by V. They modify the effective hopping, but their effects are not as strong as Eq. (6.21a) for small t.

The latter conjecture is supported by our semiclassical method. Because the prefactor $\hbar JK$ is affected little by repulsions, we show the absolute value of the exponent $W_2(E_{\rm HF})/(2\hbar)$. The on-site repulsion U decreases $W_2(E_{\rm HF})/(2\hbar)$ much more weakly than $2(\lambda t - U)/\omega$ [Fig. 10(a)]. Meanwhile, the nearest-neighbor repulsion V increases it [Fig. 10(b)]. Though the effects of electron-electron interactions are small for large λ, U enhances the tunneling of the kink and V suppresses it, because U weakens the binding of bipolarons and V strengthens it.

VII. SUMMARY AND DISCUSSION

We present a semiclassical method for many-body systems with electrons and phonons based on an overcomplete set of Slater determinants for electrons, in which single-particle wave functions satisfy the orthonormality condition (4.11) and are otherwise arbitrary. Small fluctuations around the stable static mean-field solution describe the same excitation modes as in the inhomogeneous HF plus RPA. Bosonization is effectively achieved by linearization of the orthonormality condition for single-particle wave functions.

For the 1D extended Peierls-Hubbard model near half filling, we numerically solved the imaginary-time-dependent mean-field equations and integrated over small fluctuations around the instanton solution in order to evaluate the effective hopping strength of a self-trapped kink connecting the degenerate CDW phases. The method is easily extended to more complex systems. (For the grand partion function at finite temperature, Slater determinants may not always be convenient.) At strong coupling, where tunneling of the kink involves essentially a single bipolaron, the semiclassical method reproduces the strong-coupling result for a bipolaron. It gives repulsion-strength dependences, which have not been treated with sufficient accuracy. At weak coupling, the kink is delocalized with a finite coherent length. The potential barrier is not given by the dissociation energy of a single bipolaron, but it is determined in a more collective manner.

In numerical solutions, we did not constrain the shape of classical paths, i.e., the phonon dynamics relative to the electronic one. The lattice variables evolve on a time scale different from the charge density. We observed how their evolutions vary with the bare phonon frequency and the electron-phonon coupling strength. Apart from the semiclassical study, we numerically obtained variational wave functions, through generalized Lang-Firsov-type and squeezing transformations, to observe a correlation between electrons and phonons. Both the semiclassical and variational studies show that the lattice motion follows the motion of the charge density more closely for smaller g, i.e., for larger ω if λ is kept constant; and for smaller λ if ω is kept constant. The phonon dynamics relative to the electronic one is roughly determined by a single parameter g. This parameter g determines the exponent of the effective hopping at large g. The semiclassical method is thus useful in the sense that it enables us to see the correlation between different degrees of freedom directly.

When the barrier height is more than some fraction of t or ω, the instanton density per unit imaginary time, $t_{\rm eff}/\hbar$, is so small that the dilute-instanton-gas approximation is valid. The dispersion relation of the kink is therefore described by the tight-binding model. On the other hand, when the barrier is negligible, a continuum approximation in space becomes relevant. The dispersion relation of the kink would be described, up to some maximum momentum, by a free-particle model of mass determined by a collective coordinate method as in field theories (Chap. 8 of Ref. 11).

Finally, we mention spin coherent states. They are very useful in spin tunneling problems.[34] At half filling, the Slater determinants used in this work contain the spin coherent states in the limit of single occupancy on every site. In this limit, the second term in the integrand of Eq. (2.14) becomes the corresponding term for the the spin coherent states,[35] as it should be. Slater determinants would be useful when itineracy of electrons needs to be considered, e.g., when a hole is introduced into an antiferromagnet. Once electronic degrees of freedom are split into localized spins and mobile holes,[4] it can be inaccurate when magnetic moments are locally suppressed. When the spin polaron accompanies a local lattice distortion and locally quenched magnetic moments,[17,36] the scenario of its effective hopping[4] may be altered.

ACKNOWLEDGMENTS

The author is very grateful to Lu Yu and Zhao-Bin Su for valuable discussions and enlightening comments, A. R. Bishop for his continuous encouragement and kind hospitality at Los Alamos, and C. Castellani for his comment on the continuum limit in the functional integral.

APPENDIX A: QUANTIZATION CONDITION

We consider the trace of the resolvent operator (3.4), where the paths are periodic in time t for $-T/2 < t < T/2$. The stationary phase condition leads to the time-dependent mean-field equations (3.1) with the boundary conditions

$$\phi_\gamma^-\left(i, \frac{T}{2}\right) = e^{-i\alpha_\gamma}\phi_\gamma^-\left(i, -\frac{T}{2}\right) , \tag{A1}$$

where α_γ is a path-dependent real number, and

$$u_l\left(\frac{T}{2}\right) = u_l\left(-\frac{T}{2}\right) . \tag{A2}$$

Note that the phase factor $e^{-i\alpha_\gamma}$ should be kept above since we have fixed the phase of $|\phi^-(t)\rangle$ in Eqs. (3.1). If we took $\psi_\gamma^-(i,t) = e^{i\epsilon_\gamma t/\hbar}\phi_\gamma^-(i,t)$ as a variable instead, the phase would appear in the mean-field equation, but not in the boundary condition. The quantity α_γ thus corresponds to $\epsilon_\gamma T/\hbar$. The occupied single-particle states are those of the lowest α_γ's. In real time, it is convenient to set

$$\phi_\gamma^{+*}\left(i,\frac{T}{2}\right) = \phi_\gamma^{-*}\left(i,\frac{T}{2}\right) , \tag{A3}$$

to fix the relative phase. The stationary phase condition with respect to the boundary value, $u_l(\frac{T}{2}) = u_l(-\frac{T}{2})$, yields

$$p_l\left(\frac{T}{2}\right) = p_l\left(-\frac{T}{2}\right) . \tag{A4}$$

In the evolution in *real* time t, it can be shown[14] that

$$\phi_\gamma^{+*}(i,t) = \phi_\gamma^{-*}(i,t) , \tag{A5a}$$

$$\rho(t)_{ij} = \rho(t)^*_{ji} , \tag{A5b}$$

$$u_l(t) = u_l^*(t) , \tag{A5c}$$

$$p_l(t) = p_l^*(t) , \tag{A5d}$$

and the HF matrix (3.2) is Hermitian.

The classical contribution to the action $S_c(T)$ is given by substitution of the mean-field solution into Eq. (2.14). For a given E, the period T is determined through the stationary phase condition with respect to T,

$$E = -\frac{dS_c(T)}{dT} = E_{\rm HF}(T) . \tag{A6}$$

The HF total energy $E_{\rm HF}(T)$ is given by substituting the mean-field solution into Eq. (2.15) and is independent of time. Here, the fact is used that the time derivative of the last term in Eq. (2.14),

$$-i\hbar \ln\left[\det\left\langle \phi_F \middle| \phi^-\left(\frac{T}{2}\right)\right\rangle\right] = -\hbar\sum_{\gamma\in{\rm occ}}\alpha_\gamma , \tag{A7}$$

cancels a term from the second term in the integrand of Eq. (2.14). If $T = T(E)$ is a solution of Eq. (A6), so is $nT(E)$ for any positive integer n. Summing up contributions from the multiperiod solutions produces poles of $G(E)$ at

$$W(E) \equiv S_c[T(E)] + ET(E) = 2m\pi\hbar , \tag{A8}$$

for any non-negative integer m, *if* the phase arising from fluctuations around the turning points is neglected. The phase modifies the quantization condition in such a way as should be due to the zero-point lattice fluctuations [see Eqs. (B21b) and (D1) below]. The quantity $W(E)$ can be written as

$$W(E) = \int_{-\frac{T}{2}}^{\frac{T}{2}} dt\left(\sum_l p_l(t)\frac{\partial}{\partial t}u_l(t) + \sum_{i,\gamma\in{\rm occ}}\overline{\phi_\gamma^{+*}}(i,t)i\hbar\frac{\partial}{\partial t}\phi_\gamma^-(i,t)\right) - \hbar\sum_{\gamma\in{\rm occ}}\alpha_\gamma . \tag{A9}$$

It has contributions from the lattice motion (the first term in the parentheses) and the electronic motion (the rest). The electronic contribution is not always negligible even in the adiabatic limit: it is crucial when a geometrical phase[37] arises.[31]

APPENDIX B: SMALL-AMPLITUDE FLUCTUATIONS

We consider small fluctuations around the stable *static* mean-field solution, extending Ref. 22 to interacting electron-phonon systems. Because $\phi_\gamma^{+*}(i,t) = \phi_\gamma^{-*}(i,t)$ in real time, we here rewrite $\phi_\gamma^{+*}(i,t)$ and $\phi_\gamma^-(i,t)$ as $\phi_\gamma^*(i,t)$ and $\phi_\gamma(i,t)$, respectively. We take orthonormal wave functions in the Slater determinants and set $\hbar = 1$. The variables are expanded around the static solution denoted with superscript 0,

$$\phi_\gamma(i,t) = e^{-i\epsilon_\gamma t}[\psi_\gamma^0(i) + \eta_\gamma(i,t)] , \tag{B1a}$$

$$u_l(t) = u_l^0 + v_l(t) , \tag{B1b}$$

$$p_l(t) = q_l(t) , \tag{B1c}$$

where

$$\eta_\gamma(i,t) = \sum_{\alpha\in{\rm unocc}}\psi_\alpha^0(i)C_{\alpha\gamma}(t) + \sum_{\beta\in{\rm occ}}\psi_\beta^0(i)Q_{\beta\gamma}(t) , \tag{B2a}$$

$$v_l(t) = \sum_\nu \frac{1}{\sqrt{2M_l\Omega_\nu}}\Gamma_\nu(l)[C_\nu(t) + C_\nu^*(t)] , \tag{B2b}$$

$$q_l(t) = \sum_\nu \sqrt{\frac{M_l\Omega_\nu}{2}}\Gamma_\nu(l)[-iC_\nu(t) + iC_\nu^*(t)] , \tag{B2c}$$

with Ω_ν and $\Gamma_\nu(l)$ being the eigenfrequency and eigenfunction of the bare phonon,

$$\sum_m \frac{1}{\sqrt{M_l}}K_{lm}\frac{1}{\sqrt{M_m}}\Gamma_\nu(m) = \Omega_\nu^2\Gamma_\nu(l) . \tag{B3}$$

The quantity $\eta_\gamma(i,t)$ is expanded with the use of the orthonormal wave functions $\psi_\gamma^0(i)$, which are classified into

the unoccupied ($\alpha \in$ unocc) and occupied ($\beta \in$ occ) ones according to the HF eigenvalues, $\epsilon_\alpha > \epsilon_\beta$. From the orthonormality condition, the "hole-hole amplitude" $Q_{\gamma\gamma'}(t)$ is shown to be of second order with respect to the "particle-hole amplitude" $C_{\alpha\gamma}(t)$,

$$Q_{\gamma\gamma'}(t) = -\frac{1}{2} \sum_{\alpha \in \text{unocc}} C^*_{\alpha\gamma}(t) C_{\alpha\gamma'}(t) \,, \tag{B4}$$

and neglected in the first order. Assuming a single mode of frequency ω,

$$C_{\alpha\gamma}(t) = X_{\alpha\gamma} e^{-i\omega t} + Y^*_{\alpha\gamma} e^{i\omega t} \,, \tag{B5a}$$

$$C_{\nu}(t) = X_{\nu} e^{-i\omega t} + Y^*_{\nu} e^{i\omega t} \,, \tag{B5b}$$

and substituting the above into Eqs. (3.1), we get the RPA equation [(B6) of Ref. 17]:

$$\begin{pmatrix} \Omega + K_A & K_B \\ K_B^* & \Omega + K_A^* \end{pmatrix} \begin{pmatrix} X \\ Y \end{pmatrix} = \omega \begin{pmatrix} X \\ -Y \end{pmatrix} \,, \tag{B6}$$

where the vector denotes

$$X = \begin{pmatrix} X_{\alpha\beta} \\ X_\gamma \end{pmatrix} \,, \quad Y = \begin{pmatrix} Y_{\alpha\beta} \\ Y_\gamma \end{pmatrix} \,, \tag{B7}$$

with α unoccupied and β occupied. The quantities Ω, K_A, and K_B are the same as in Ref. 17, while X and Y here correspond to ψ^* and φ^* there, respectively.

For the mode n of frequency ω_n, the period T_n must satisfy $\omega_n T_n = 2m\pi$ for an integer m. The phase $\alpha_\gamma^{(n)}$ is given by $\alpha_\gamma^{(n)} = \epsilon_\gamma T_n$. With the use of these equations, substitution of Eqs. (B1) into Eq. (A9) leads to the normalization condition, (B13) of Ref. 17. The equations above are straightforward generalizations of those in Ref. 22.

Below we will derive the total energy. It has not explicitly been derived with the Slater-determinant representation because a continuum limit is ill defined. We will show how to handle it to get the correct result. The classical contribution to the action $S_c(T)$ is given by

$$S_c(T) = -E_{\text{HF}} T \,, \tag{B8}$$

where E_{HF} is independent of the period T. The linear term with respect to fluctuations vanishes because of the stationary phase condition. Therefore, there is no term linear in $Q_{\beta\gamma}(t)$ or $Q^*_{\beta\gamma}(t)$. In the second order, we only have to retain terms which are bilinear with respect to $C_{\alpha\gamma}(t)$ and $C^*_{\alpha\gamma}(t)$:

$$S_q(T) = \frac{1}{2} \int_{-\frac{T}{2}}^{\frac{T}{2}} dt dt' \left[\, C^\dagger(t) \tilde{C}(t) \, \right] \times \left\{ [\Pi(t)]^{-1} \delta \right\} \begin{pmatrix} C(t') \\ C^*(t') \end{pmatrix} \,, \tag{B9}$$

where $\delta = \delta(t - t')$,

$$[\Pi(t)]^{-1} = \begin{pmatrix} i\frac{\partial}{\partial t} - \Omega - K_A & -K_B \\ -K_B^* & -i\frac{\partial}{\partial t} - \Omega - K_A^* \end{pmatrix} \,, \tag{B10}$$

the vector $C(t)$ denotes

$$C(t) = \begin{pmatrix} C_{\alpha\beta}(t) \\ C_\gamma(t) \end{pmatrix} \,, \tag{B11}$$

and $\tilde{C}(t)$ its transpose. The Fourier transform of the quantity $\Pi(t)$ is the same as that in (C1) of Ref. 17 [see (C4), (C6), and (C7) there]. Note that $C_{\alpha\gamma}(t)$, $C^*_{\alpha\gamma}(t)$, $Q_{\beta\gamma}(t)$, and $Q^*_{\beta\gamma}(t)$ are not independent because of the orthonormality condition. But the orthonormality condition for the integration variables $\phi_\gamma(i,t)$ and $\phi^*_\gamma(i,t)$ needs to be satisfied to first order. In other words, integrations over $Q_{\beta\gamma}(t)$ and $Q^*_{\beta\gamma}(t)$ are suppressed and those over $C_{\alpha\gamma}(t)$ and $C^*_{\alpha\gamma}(t)$ should be performed. The measure is thus written as

$$\mathcal{D}(C^*_{\alpha\beta}(t), C^*_\gamma(t), C_{\alpha\beta}(t), C_\gamma(t)) = \frac{1}{\mathcal{N}} \prod_{k=1}^{L} \left[\prod_{\alpha,\beta} dC^*_{\alpha\beta}(t_k) dC_{\alpha\beta}(t_k) \prod_{\gamma} dC^*_\gamma(t_k) dC_\gamma(t_k) \right] \,. \tag{B12}$$

The trace of the resolvent operator is thus evaluated through Gaussian integration as

$$\begin{aligned} G(E) &\simeq -i \int_0^\infty dT e^{iET - iE_{\text{HF}}T} \int \mathcal{D}(C^*_{\alpha\beta}(t), C^*_\gamma(t), C_{\alpha\beta}(t), C_\gamma(t)) \\ &\quad \times \exp\left[\frac{i}{2} \int_{-\frac{T}{2}}^{\frac{T}{2}} dt dt' \left[\, C^\dagger(t) \tilde{C}(t) \, \right] \left\{ [\Pi(t)]^{-1} \delta \right\} \begin{pmatrix} C(t') \\ C^*(t') \end{pmatrix} \right] \\ &= -i \int_0^\infty dT e^{iET - iE_{\text{HF}}T} \frac{1}{\mathcal{N}} \left(\det \left\{ -i[\Pi(t)]^{-1} \delta \right\} \right)^{-1/2} \,, \end{aligned} \tag{B13}$$

where the normalization constant $\mathcal{N}$ subtracts the vacuum energy from the exponent of the integrand. We can write the constant as

$$\mathcal{N} = \left(\det \left\{ -i[\Pi_0(t)]^{-1} \delta \right\} \right)^{-1/2} \,, \tag{B14}$$

with the noninteracting polarization $\Pi_0(t)$ given by

$$[\Pi_0(t)]^{-1} = \begin{pmatrix} i\frac{\partial}{\partial t} - \Omega & 0 \\ 0 & -i\frac{\partial}{\partial t} - \Omega \end{pmatrix} \,. \tag{B15}$$

From the middle of Eq. (B13) and the property of Gaussian integrals, it is easily understood that elements of $\Pi(t)$ are nothing but response functions.

With the use of

$$\Pi_0(t)[\Pi(t)]^{-1} = 1 - \Pi_0(t)K \ , \tag{B16}$$

where

$$K = \begin{pmatrix} K_A & K_B \\ K_B^* & K_A^* \end{pmatrix} \ , \tag{B17}$$

we rewrite the determinant as

$$\begin{aligned} &\frac{1}{\mathcal{N}}\left(\det\left\{-i[\Pi(t)]^{-1}\delta\right\}\right)^{-1/2} \\ &\quad = \left(\det\left\{\Pi_0(t)[\Pi(t)]^{-1}\delta\right\}\right)^{-1/2} \\ &\quad = \exp\left(-\tfrac{1}{2}\mathrm{tr}\left\{\ln[1-\Pi_0(t)K\delta]\right\}\right) \\ &\quad = \exp\left[-iT\int_{-\infty}^{\infty}\frac{d\omega}{4\pi i}\mathrm{tr}\left\{\ln[1-\Pi_0(\omega)K]\right\}\right] \ . \end{aligned} \tag{B18}$$

Here the symbol tr inside the frequency integral denotes summation over $\alpha\beta$, γ, $\alpha\beta^*$, and γ^* components, while the other tr symbol takes summation over time components as well. The integrand can be expanded with respect to K as

$$\begin{aligned} &\int_{-\infty}^{\infty}\frac{d\omega}{4\pi i}\mathrm{tr}\left\{\ln[1-\Pi_0(\omega)K]\right\} \\ &\qquad = -\int_{-\infty}^{\infty}\frac{d\omega}{4\pi i}\sum_{m=1}^{\infty}\frac{1}{m}\mathrm{tr}\left[\Pi_0(\omega)K\right]^m \ . \end{aligned} \tag{B19}$$

The first-order term ($m = 1$) in the integrand behaves like $1/\omega$ as $|\omega| \to \infty$ so that care must be taken. In the ordinary perturbation theory, a factor $e^{i\omega 0^{\pm}}$ specifies the correct order of creation and annihilation operators and determines how the integration contour is closed.

Let us go back to the discrete-time representation for $\Pi_0(t)$ in order to keep the correct order and to see how the contour should be closed.[38] The noninteracting electronic part of $S_q(T)$ is

$$\begin{aligned} &\epsilon\sum_k\sum_{\alpha\beta}\left[C^*_{\alpha\beta}(t_k)i\frac{C_{\alpha\beta}(t_k)-C_{\alpha\beta}(t_{k-1})}{\epsilon} - C^*_{\alpha\beta}(t_k)(\epsilon_\alpha-\epsilon_\beta)C_{\alpha\beta}(t_{k-1})\right] \\ &\qquad \simeq \epsilon'\sum_\nu\sum_{\alpha\beta}C^*_{\alpha\beta}(\omega_\nu)\left[i\frac{1-e^{i\omega_\nu\epsilon}}{\epsilon} - (\epsilon_\alpha-\epsilon_\beta)e^{i\omega_\nu\epsilon}\right]C_{\alpha\beta}(\omega_\nu) \ , \end{aligned}$$

where ϵ is the width of a time slice and ϵ' of a frequency slice. The particle-hole component of $\Pi_0(\omega)$ is thus given by the $\epsilon \to 0$ limit of

$$\left[i\frac{1-e^{i\omega\epsilon}}{\epsilon} - (\epsilon_\alpha-\epsilon_\beta)e^{i\omega\epsilon}\right]^{-1} \ .$$

The contour should be closed in the lower half plane while the pole is in the upper half plane. Therefore, the first-order term ($m = 1$) vanishes. The frequency integration is performed as in Sec. 15.9 of Ref. 14:

$$\begin{aligned} &-\int_{-\infty}^{\infty}\frac{d\omega}{4\pi i}\sum_{m=2}^{\infty}\frac{1}{m}\mathrm{tr}\left[\Pi_0(\omega)K\right]^m \\ &\qquad = \frac{1}{2}\sum_{n;\omega_n>0}\omega_n - \frac{1}{2}\mathrm{tr}(\Omega+K_A) \ , \end{aligned} \tag{B20}$$

where ω_n is the eigenvalue of the nth mode in Eq. (B6). Among the pairs of positive and negative eigenvalues with the same magnitude, $\pm\omega_n$ ($\omega_n \geq 0$), only the positive ones are summed in the first term.

Finally, from Eqs. (B13) and (B18)–(B20), we get

$$G(E) \simeq \left[E - \left(E_{\mathrm{HF}} + \frac{1}{2}\sum_{n;\omega_n>0}\omega_n - \frac{1}{2}\mathrm{tr}(\Omega+K_A)\right)\right]^{-1} \ . \tag{B21a}$$

If the fluctuations around the turning points were included, this would be replaced by

$$\begin{aligned} G(E) \simeq \Bigg[E - \Bigg(&E_{\mathrm{HF}} + \frac{1}{2}\sum_\nu\Omega_\nu \\ &+\frac{1}{2}\sum_{n;\omega_n>0}\omega_n - \frac{1}{2}\mathrm{tr}(\Omega+K_A)\Bigg)\Bigg]^{-1} \ , \end{aligned} \tag{B21b}$$

which has a pole at the RPA total energy (but with double counting of the second-order term with respect to the electron-electron interaction). It should be noted that, if coherent states are used to describe phonon states after the second quantization (i.e., after the lattice variables are regarded as operators and written with the use of creation and annihilation operators), the bare zero-point lattice energy is included at the "classical" level.

APPENDIX C: NUMERICAL DETAILS

Equation (4.4a) was solved in such a way as taken in Appendix D of Ref. 16. The wave functions are evolved discretely from τ to $\tau+\Delta\tau$ through the HF matrix at the intermediate time $\tau+\Delta\tau/2$. In the HF matrix, the electronic one-body densities and the lattice displacements are averaged over τ and $\tau+\Delta\tau$. The periodic boundary condition (4.6) is fulfilled by the solution of an eigenvalue equation. The eigenvalues correspond to $e^{-\lambda_\gamma}$'s. One remark on the eigenvalue problem is that the matrix to be diagonalized (M_{in} in Ref. 16) is Hermitian because the HF matrices, $h[\rho(\tau),u(\tau)]$ and $h[\rho(-\tau),u(-\tau)]$, are con-

jugate. This fact and the normalization condition for the wave functions lead to the fact that λ_γ is a real number (mod $2\pi i$).

Equations (4.4c) and (4.4d) were solved by evolving the lattice variables discretely from τ to $\tau+\Delta\tau$ through the right hand sides at $\tau+\Delta\tau/2$, in which the electronic one-body densities and the lattice displacements are averaged over τ and $\tau+\Delta\tau$. The initial value $p_l(-T_2/2)$ is zero. Because of Eqs. (4.10c) and (4.10d), we only need to compute $u_l(\tau)$ and $p_l(\tau)$ from $\tau=-T_2/2$ to $\tau=0$. The boundary conditions, Eqs. (4.7) and (4.9), are automatically satisfied. The condition (4.10d) at $\tau=0$ determines the initial value, $u_l(-T_2/2)$.

Iteration is performed as follows. First, some values are assigned to "old" values for $\rho(\tau)_{ij}$ and $u_l(\tau)$ to define $h(\tau)$ and $F_l(\tau)$. These "old" values can be taken from "new" values in the previous step. But it is better to mix "new" values in the last, e.g., two steps to slow down changes between successive iteration steps and to suppress possible oscillations of these quantities. To simplify the explanation below, we suppose here that the "new" values are chosen to be the "old" values in the next step.

The electronic wave functions are evolved through $h(\tau)$ till $\tau=T_2/2$, as described above. Then "new" $\rho(\tau)_{ij}$ can be obtained from these "new" wave functions as shown in Eq. (4.12). The 'new' $p_l(\tau)$ can be obtained by adding $F_l(\tau)$ to the zero initial value. The initial value of 'new' $u_l(-T_2/2)$ is unknown at this moment. So, let us take the initial value of the "old" $u_l(-T_2/2)$ for that. Then a 'new' $u_l(\tau)$ can be obtained by adding the 'new' $p_l(\tau)$ divided by the mass. The real part of the 'new' $p_l(0)$ becomes zero only if the appropriate initial value is chosen for the "new" $u_l(-T_2/2)$. Note that we have distinguished 'new' from "new" here.

Second, the "new" $\rho(\tau)_{ij}$ and the 'new' $u_l(\tau)$ are used to define a 'new' $F_l(\tau)$. Then a temporarily defined $p_l(\tau)$ is obtained by adding the 'new' $F_l(\tau)$ to the zero initial value. This generally leads to a finite value for the real part of the temporarily defined $p_l(0)$. The correct "new" $u_l(\tau)$ would be obtained by adding a site-dependent, time-independent, real-number constant to the 'new' $u_l(\tau)$. When site-dependent constants were added to the 'new' $u_l(\tau)$ values, the 'new' $F_l(\tau)$ and the temporarily defined $p_l(\tau)$ values are changed linearly. Therefore, the appropriate real constants are easily obtained from the temporarily defined $p_l(0)$ so that the "new" $u_l(\tau)$ leads the real part of the "new" $p_l(0)$ to be zero. It should be noted that, in this second process, $u_l(\tau)$ does not need to be evolved again.

The above iteration process is repeated until convergent $\rho(\tau)_{ij}$ and $u_l(\tau)$ are obtained. In the iteration process, we actually imposed a constraint in order not to change time-averaged "old" $\rho(\tau)_{ij}$ and/or $u_l(\tau)$ values near the kink between two successive iteration steps. Otherwise, $\rho(\tau)_{ij}$ and $u_l(\tau)$ change violently as iteration proceeds, and the configuration finally reaches a *stable* static mean-field solution as observed in Ref. 16. (If T_2 is smaller than a critical value T_{2c}, the configuration always reaches an *unstable* static mean-field solution at the top of a barrier.) This instability is related to the fact that we are searching not a local extremum but a saddle point: there is always an unstable mode around a bounce solution. Even if iteration started from very near the solution, the configuration would deviate from it without a constraint.

Because of the constraint, the (mixed) "new" values are generally not the "old" values. We first obtained convergent $\rho(\tau)_{ij}$ and $u_l(\tau)$ with a few different constraints by the ordinary iteration method. We changed the constraint through the Newton method in such a way that the convergent constraint makes "new" and "old" time-averaged quantities equal. This process converges very rapidly in several Newton-method steps.

APPENDIX D: DISCRETE-TIME REPRESENTATION

Because a continuum limit is ill defined, the discrete-time representation should be used for calculations of the determinants. As mentioned in Appendix B, the discrete-time representation keeps the correct order of creation and annihilation operators. We will use here the coherent-state representation for phonons. Wave functions of electrons and phonons are represented in a similar manner. This representation actually changes the ordering of phonon variables with respect to time (see below). Symbolically, the oscillation of the lattice coordinates and momenta, $q(t)=\sqrt{1/(2M\Omega)}[\phi(t)+\phi^*(t)]$ and $p(t)=\sqrt{M\Omega/2}[-i\phi(t)+i\phi^*(t)]$, is described by the rotation of the coherent-state variables $\phi(t)$ and $\phi^*(t)$. Thus, the mathematical difficulty caused by the turning points disappears. The bare zero-point lattice energy emerging from the turning points is actually included at the classical level since the variables $\phi(t)$ and $\phi^*(t)$ are introduced after the second quantization. Therefore, the time ordering with respect to $\phi(t)$ and $\phi^*(t)$ is more convenient. The quantity $W(E)$ is to be replaced by

$$W(E)=\int_{-\frac{T}{2}}^{\frac{T}{2}}dt\left(\sum_\nu \overline{\phi_\nu^{+*}}(t)i\hbar\frac{\partial}{\partial t}\phi_\nu^-(t)+\sum_{i,\gamma\in\mathrm{occ}}\overline{\phi_\gamma^{+*}}(i,t)i\hbar\frac{\partial}{\partial t}\phi_\gamma^-(i,t)\right)-\hbar\sum_{\gamma\in\mathrm{occ}}\alpha_\gamma\,, \tag{D1}$$

where $\phi_\nu^-(t)$ and $\overline{\phi_\nu^{+*}}(t)=\phi_\nu^{+*}(t)$ are for the mode ν of the bare phonon. Inclusion of the bare zero-point lattice energy should be understood for quantization.

Repeated insertion of the closure relation

$$1\propto\prod_\nu\prod_{i,\gamma\in\mathrm{occ}}\int d\phi_\nu^{+*}(t_k)d\phi_\nu^-(t_k)d\phi_\gamma^{+*}(i,t_k)d\phi_\gamma^-(i,t_k)e^{-\sum_\nu\phi_\nu^{+*}(t_k)\phi_\nu^-(t_k)-\sum_{i,\gamma\in\mathrm{occ}}\phi_\gamma^{+*}(i,t_k)\phi_\gamma^-(i,t_k)}|\Phi_k^-\rangle\langle\Phi_k^+|\,, \tag{D2}$$

for $k = 1, \ldots, L/2$ $(-T_2/2 < \tau < 0)$ in the Trotter formula leads to the Euclidean action

$$S_E[\Phi^{+*}(\tau), \Phi^-(\tau)] = \epsilon \sum_{k=1}^{L/2} \Bigg[\sum_\nu \overline{\phi_\nu^{+*}}(\tau_k) \frac{\phi_\nu^-(\tau_k) - \phi_\nu^-(\tau_{k-1})}{\epsilon} + \sum_{i,\gamma \in \mathrm{occ}} \overline{\phi_\gamma^{+*}}(i,\tau_k) \frac{\phi_\gamma^-(i,\tau_k) - \phi_\gamma^-(i,\tau_{k-1})}{\epsilon} + \mathcal{H}[\Phi^{+*}(\tau_k), \Phi^-(\tau_{k-1})] \Bigg] - \ln\left[\det\langle \phi_F | \phi^-(0)\rangle\right] , \tag{D3}$$

where

$$\mathcal{H}[\Phi^{+*}(\tau_k), \Phi^-(\tau_{k-1})] = \sum_{i,j} \left[T_{ij}^0 + \sum_\nu g_{ij}^\nu [\phi_\nu^-(\tau_{k-1}) + \overline{\phi_\nu^{+*}}(\tau_k)] \right] \rho(\tau_{k-\frac{1}{2}})_{ji} + \frac{1}{2} \sum_{i,j,l,m} \{il|V|jm\} \rho(\tau_{k-\frac{1}{2}})_{ji} \rho(\tau_{k-\frac{1}{2}})_{ml} + \sum_\nu \Omega_\nu [\overline{\phi_\nu^{+*}}(\tau_k) \phi_\nu^-(\tau_{k-1}) + \tfrac{1}{2}] , \tag{D4}$$

with $\rho(\tau_{k-\frac{1}{2}})_{ij} = \sum_{\gamma \in \mathrm{occ}} \phi_\gamma^-(i,\tau_{k-1}) \overline{\phi_\gamma^{+*}}(j,\tau_k)$, $T_{ij}^0 = T_{ij}(\{u_m = 0\})$, and

$$g_{ij}^\nu = \sum_l \bar{g}_{ij}^l \frac{1}{\sqrt{2M_l\Omega_\nu}} \Gamma_\nu(l) . \tag{D5}$$

For phonons, we used the notation $\phi_\nu^-(\tau) = \phi_\nu^-(t = -i\tau)$, $\overline{\phi_\nu^{+*}}(\tau) = \overline{\phi_\nu^{+*}}(t = -i\tau)$.

We consider fluctuations (5.1a), (5.1b), (5.2a), and (5.2b) for electronic wave functions at each discrete time, and

$$\phi_\nu^-(\tau_{k-1}) = \phi_\nu^0(\tau_{k-1}) + C_\nu(\tau_{k-1}) , \tag{D6a}$$

$$\overline{\phi_\nu^{+*}}(\tau_k) = \overline{\phi_\nu^{*}}^0(\tau_k) + \overline{C_\nu^*}(\tau_k) , \tag{D6b}$$

where $\phi_\nu^0(\tau)$ and $\overline{\phi_\nu^*}^0(\tau)$ denote the classical lattice trajectory related to $u_l^0(\tau)$ and $p_l^0(\tau)$ by

$$u_l^0(\tau) = \sum_\nu \frac{1}{\sqrt{2M_l\Omega_\nu}} \Gamma_\nu(l) [\phi_\nu^0(\tau) + \overline{\phi_\nu^*}^0(\tau)] , \tag{D7a}$$

$$p_l^0(\tau) = \sum_\nu \sqrt{\frac{M_l\Omega_\nu}{2}} \Gamma_\nu(l) [-\phi_\nu^0(\tau) + \overline{\phi_\nu^*}^0(\tau)] . \tag{D7b}$$

Note the factor $-i$ in Eq. (4.1d). The quadratic term $S_{Eq}[\overline{C^*}(\tau), C(\tau); T_2/2]$ is obtained in a straightforward manner,

$$S_{Eq}\left[\overline{C^*}(\tau), C(\tau); \frac{T_2}{2}\right] = \frac{1}{2} \sum_{k,k'=1}^{L/2} [\, \overline{C^\dagger}(\tau_k) \tilde{C}(\tau_k) \,] \left[\Pi_E\left(\tau_k, \tau_{k'}; \frac{T_2}{2}\right)\right]^{-1} \begin{pmatrix} C(\tau_{k'}) \\ \overline{C^*}(\tau_{k'}) \end{pmatrix}$$
$$\equiv \frac{1}{2} \sum_{k=1}^{L/2} \Bigg[\sum_{\alpha,\beta} \{\overline{C_{\alpha\beta}^*}(\tau_k)[C_{\alpha\beta}(\tau_k) - C_{\alpha\beta}(\tau_{k-1})] + [C_{\alpha\beta}(\tau_k) - C_{\alpha\beta}(\tau_{k-1})]\overline{C_{\alpha\beta}^*}(\tau_k)\}$$
$$+ \sum_\gamma \{\overline{C_\gamma^*}(\tau_k)[C_\gamma(\tau_k) - C_\gamma(\tau_{k-1})] + [C_\gamma(\tau_k) - C_\gamma(\tau_{k-1})]\overline{C_\gamma^*}(\tau_k)\} + \epsilon \, [\, \overline{C^\dagger}(\tau_k) \;\; \tilde{C}(\tau_{k-1}) \,]$$
$$\times \begin{pmatrix} \bar{\Omega} + K_A(\tau_{k-\frac{1}{2}}) & K_B(\tau_{k-\frac{1}{2}}) \\ K_B^*(-\tau_{k-\frac{1}{2}}) & \bar{\Omega} + K_A^*(-\tau_{k-\frac{1}{2}}) \end{pmatrix} \begin{pmatrix} C(\tau_{k-1}) \\ \overline{C^*}(\tau_k) \end{pmatrix} \Bigg] , \tag{D8}$$

with the boundary condition

$$C(\tau_0) = \overline{C^*}(\tau_{L/2}) = 0 . \tag{D9}$$

The above equation defines the quantity $\Pi_E(\tau_k, \tau_{k'}; \frac{T_2}{2})$. Here $K_A(\tau_{k-\frac{1}{2}})$ and $K_B(\tau_{k-\frac{1}{2}})$ are approximated as $[K_A(\tau_k) + K_A(\tau_{k-1})]/2$ and $[K_B(\tau_k) + K_B(\tau_{k-1})]/2$, respectively. Finally, the contribution of one instanton to the right hand side of Eq. (4.2b) is given by

$$\exp\left(-E_{\mathrm{HF}}(T_2)\frac{T_2}{2} - \frac{1}{2}W_2[E_{\mathrm{HF}}(T_2)]\right) \times \frac{|\det[\Pi_E(\tau_k, \tau_{k'}; \frac{T_2}{2})^{-1}]|^{-1/2}}{|\det[\Pi_{E0}(\tau_k, \tau_{k'}; \frac{T_2}{2})^{-1}]|^{-1/2}} . \tag{D10}$$

A special treatment is necessary for the zero mode. In analytic treatments in field theories, a Jacobian is needed for the transformation from the zero-mode coordinate to a collective coordinate. In our numerical treatment, however, the zero mode has a finite eigenvalue because T_2 is finite. Consequently, the quantity $T_2/2$ is easily factored out from (D10) as

$$\frac{|\det[\Pi_E(\tau_k, \tau_{k'}; \frac{T_2}{2})^{-1}]|^{-1/2}}{|\det[\Pi_{E0}(\tau_k, \tau_{k'}; \frac{T_2}{2})^{-1}]|^{-1/2}} = JK\frac{T_2}{2} . \tag{D11}$$

The product JK is obtained numerically by dividing the quantity on the left hand side by $T_2/2$ and taking the $T_2 \to \infty$ limit.

* Present address: Center for Simulational Physics, Department of Physics and Astronomy, University of Georgia, Athens, GA 30602.
[1] K. Yonemitsu and A. R. Bishop, Phys. Rev. B **45**, 5530 (1992).
[2] J. Lorenzana, M. Grynberg, L. Yu, K. Yonemitsu, and A. R. Bishop, Phys. Rev. B **47**, 13 156 (1993).
[3] K. Yonemitsu, A. R. Bishop, and J. Lorenzana, Mod. Phys. Lett. B **7**, 355 (1993).
[4] A. Auerbach and B. E. Larson, Phys. Rev. Lett. **66**, 2262 (1991); A. Auerbach, Phys. Rev. B **48**, 3287 (1993).
[5] S. Coleman, Phys. Rev. D **15**, 2929 (1977).
[6] A. S. Ioselevich and E. I. Rashba, in *Quantum Tunneling in Condensed Media*, edited by Yu. Kagan and A. J. Leggett (North-Holland, Amsterdam, 1992).
[7] V. V. Kabanov and O. Yu. Mashtakov, Phys. Rev. B **47**, 6060 (1993).
[8] K. Maki, Phys. Rev. B **18**, 1641 (1978).
[9] A. Terai and Y. Ono, Prog. Theor. Phys. Suppl. **113**, 177 (1993), and references therein.
[10] S. Coleman, in *The Whys of Subnuclear Physics*, edited by A. Zichichi (Plenum, New York, 1979).
[11] R. Rajaraman, *Solitons and Instantons* (North-Holland, Amsterdam, 1982).
[12] J. W. Negele, Rev. Mod. Phys. **54**, 913 (1982).
[13] J. W. Negele and H. Orland, *Quantum Many-Particle Systems* (Addison-Wesley, Redwood City, CA, 1988), Chap. 7.
[14] J.-P. Blaizot and G. Ripka, *Quantum Theory of Finite Systems* (MIT Press, Cambridge, 1986), Secs. 9.1a, 9.4, and 11.8.
[15] S. Levit, Phys. Rev. C **21**, 1594 (1980).
[16] S. Levit, J. W. Negele, and Z. Paltiel, Phys. Rev. C **22**, 1979 (1980).
[17] K. Yonemitsu, A. R. Bishop, and J. Lorenzana, Phys. Rev. B **47**, 12 059 (1993).
[18] G. Beni, P. Pincus, and J. Kanamori, Phys. Rev. B **10**, 1896 (1974).
[19] J. E. Hirsch and E. Fradkin, Phys. Rev. B **27**, 4302 (1983).
[20] K. Yonemitsu, in *Nonlinear Coherent Structures in Physics and Biology*, edited by K. H. Spatscheck and F. G. Mertens (Plenum, New York, in press).
[21] R. F. Dashen, B. Hasslacher, and A. Neveu, Phys. Rev. D **10**, 4114 (1974).
[22] S. Levit, J. W. Negele, and Z. Paltiel, Phys. Rev. C **21**, 1603 (1980).
[23] We do not consider in this study cases where $\phi_\gamma^-(i, \frac{T_2}{2}) = e^{-\lambda}\phi_\delta^-(i, -\frac{T_2}{2})$ for $\gamma \neq \delta$, since exchanges of electrons are hardly expected due to the bipolaron formation.
[24] M. Stone, Phys. Rev. D **33**, 1191 (1986).
[25] D. Feinberg, S. Ciuchi, and F. de Pasquale, Int. J. Mod. Phys. B **4**, 1317 (1990).
[26] K. Nasu, J. Phys. Soc. Jpn. **52**, 3865 (1983); **53**, 302 (1984); **53**, 427 (1984).
[27] H. Zheng, D. Feinberg, and M. Avignon, Phys. Rev. B **39**, 9405 (1989); **41**, 11 557 (1990).
[28] H. Fehske, D. Ihle, U. Trapper, and H. Büttner (unpublished).
[29] Though $\bar{\gamma}_i$ shows an oscillatory behavior in the background as $\langle n_i \rangle$ does, $\gamma_{i\sigma}$ does not depend on i so much. For the parameter sets shown in Table I, the difference between $\gamma_{i\sigma}$ near the kink and that distant from the kink is less than a few percent.
[30] G. Delacrétaz, E. R. Grant, R. L. Whetten, L. Wöste, and J. W. Zwanziger, Phys. Rev. Lett. **56**, 2598 (1986).
[31] G. Herzberg and H. C. Longuet-Higgins, Discuss. Faraday Soc. **35**, 77 (1963); H. C. Longuet-Higgins, Proc. R. Soc. London, Ser. A **344**, 147 (1975).
[32] J. E. Hirsch, Phys. Rev. B **31**, 6022 (1985).
[33] The quantity $2g^2$ in the denominator of Eq. (6.14) comes from the energy difference between the two singly occupied sites and the empty and doubly occupied sites, $2g^2\omega = \beta^2/K$. It would be replaced by $\beta^2/K - U$ for $V = 0$. But it does not contribute to the exponent of Eq. (6.15), which is determined by the other g^2 dependence.
[34] D. Loss, D. P. DiVincenzo, and G. Grinstein, Phys. Rev. Lett. **69**, 3232 (1992); J. von Delft and C. L. Henley, *ibid.* **69**, 3236 (1992).
[35] J. R. Klauder, Phys. Rev. D **19**, 2349 (1979).
[36] K. Yonemitsu, A. R. Bishop, and J. Lorenzana, Phys. Rev. Lett. **69**, 965 (1992).
[37] M. V. Berry, Proc. R. Soc. London, Ser. A **392**, 45 (1984).
[38] C. Castellani (private communication).